Comparison of statistical iceberg forecast models☆

Leif Erik Andersson[a,*], Francesco Scibilia[a,b], Luke Copland[c], Lars Imsland[a]

[a]*Department of Engineering Cybernetics, Norwegian University of Science and Technology, 7491 Trondheim, Norway*
[b]*Statoil ASA, Statoil Research Center, Arkitekt Ebbells veg 10, 7053 Ranheim, Norway*
[c]*Department of Geography, Environment and Geomatics, University of Ottawa, Ottawa, Ontario, ON K1N 6N5, Canada*

Abstract

Short-term iceberg drift prediction is challenging. Large uncertainties in the driving forces – current, wind and waves – usually prevent accurate forecasts. Recently several statistical iceberg forecast models have been proposed by the authors, which use iceberg position measurements to improve the short-term drift forecast. In this article these statistical forecast methods and models are briefly reviewed. An extensive comparison between the statistical models, in addition to a dynamic iceberg forecast model, is performed on several iceberg drift trajectories. Based on this comparison a new statistical forecast scheme is proposed that combines some of the advantages of the other methods.

Keywords: Iceberg drift forecasting, offshore operations, parameter estimation, multivariate empirical mode decomposition, moving horizon estimator, model identification

1. Introduction

Short-term iceberg drift forecast is part of the Ice Management framework, which is a key component of the International Standard, ISO 19906, specifying requirements and guidance for the design, construction, transportation, installation and decommissioning of offshore platforms. However, predicting problematic iceberg trajectories that approach vulnerable offshore structures and development activities is still not solved to a satisfying extent. Large uncertainties in the iceberg driving forces – current, wind, waves – and in the iceberg model parameters – mass, cross-sections, drag coefficients – prevent accurate forecasts.

A simplistic mechanistic dynamic iceberg drift model was developed in the 1980's (Sodhi and El-Tahan, 1980) and further improved and tested by among others Mountain (1980); EI-Tahan et al. (1983); Smith (1993); Bigg et al. (1996); Eik (2009); Turnbull et al. (2015). An operational iceberg drift model based on a dynamic drift model was developed at the National Research Council of Canada and implemented at the Canadian Ice Service (CIS) and other agencies (Kubat et al., 2005). A similar dynamic operational model was developed to monitor ice conditions in the western Arctic by the Russian Federation (Kulakov and Demchev, 2015). The model uses environmental inputs as winds, waves and ocean currents and a detailed description of the iceberg keel geometry to simulate the iceberg drift.

Even though the main drift direction of the operational iceberg model is claimed to be satisfactory (Mountain, 1980; Kubat et al., 2005; Bigg et al., 1997), the modeled and observed iceberg trajectories may deviate from the beginning or even point in opposite directions (EI-Tahan et al., 1983). The iceberg drift segments analyzed in Smith (1993); Andersson et al. (2017b) had a duration of 6 h to 73 h, and it was observed that even if the iceberg keel shape and the ocean current close to the iceberg were measured it is not always possible to forecast or even hindcast the drift of an iceberg over short periods. Periods, which do not exceed 24 h, are referred to as short-term forecasts (Marko et al., 1988).

If an iceberg approaches an offshore installation more information (presuming more access to observations) about the iceberg trajectory becomes available. The iceberg may even be tracked continuously. In this situation approaches that include past information to forecast an iceberg trajectory may be used. For short-term forecasts of iceberg trajectories it was observed that these *statistical* models that incorporate past observations exhibit superior performance relative to the conventional mechanistic dynamic models (Andersson et al., 2016a; Marko et al., 1988).

Several statistical models were developed in the 1980's by Gaskill and Rochester (1984); De Margerie et al. (1986); Moore (1987). More recently several ideas for how to forecast an iceberg trajectory including past measurements to the forecast have been proposed (Andersson et al., 2016a,d,b, 2017a). The proposals were tested and compared to a mechanistic dynamic model on different iceberg data sets. They all have in common that they are in average superior to the mechanistic dynamic model, but a comparison among themselves was not performed for short-term iceberg drift forecasts.

This article addresses this situation by giving a brief

*Correspondence should be addressed to Leif Erik Andersson: e-mail: leif.e.andersson@ntnu.no; tel.: +47 735 94 365

introduction to the methods and attempting to make a fair comparison between the forecast performances. The weaknesses and strengths of the methods are discussed and possible combinations to improve the forecast performance are suggested.

The article is organized as follows: in Section 2 the methods and theory used in the forecast schemes are introduced, followed by a brief introduction of each statistical forecast scheme in Section 3. The iceberg, ocean current and wind data sets used during the comparison are presented in Section 4. In Section 5 performance indices to evaluate and compare the methods are proposed. The comparison of the forecast methods is given in Section 6. In Section 7 improvements of the methods and possible combinations of different methods are discussed. The article ends with a conclusion and an outlook to possible future work in Section 8.

2. Theory and Methods

In this section the methods used in the forecast schemes are briefly presented.

Hereafter, the *North-East-Down* (NED) coordinate system is used throughout the article.

When analyzing a temporal data set of iceberg positions, the following discretization of a continuous time model can be used

$$\mathbf{x}_{k+1} = \mathbf{f}(\mathbf{x}_k, \mathbf{u}_k) + \mathbf{w}_k, \quad \mathbf{x}_0 = \mathbf{x}(t_0), \tag{1a}$$

$$\mathbf{y}_k = \mathbf{h}(\mathbf{x}_k) + \mathbf{v}_k, \tag{1b}$$

in which k denotes the samples taken at a discrete time t_k. The vector $\mathbf{x}_k \in \mathbb{R}^{n_x}$, $\mathbf{u}_k \in \mathbb{R}^{n_u}$, $\mathbf{y}_k \in \mathbb{R}^{n_y}$, $\mathbf{w}_k \in \mathbb{R}^{n_x}$ and $\mathbf{v}_k \in \mathbb{R}^{n_y}$ represent the states, the inputs, the outputs, the process and the measurement noise, respectively. In the context of this paper, the state $\mathbf{x}$ is typically the two-dimensional iceberg position and velocity, $\mathbf{u}$ the environmental driving forces, $\mathbf{f}$ represents the momentum balance and $\mathbf{w}$ the process noise. The position measurements $\mathbf{y}$ is represented by the function $\mathbf{h}$ and the measurement noise $\mathbf{v}$. The process noise $\mathbf{w}$ accounts for unknown disturbances on the system states due to model uncertainty and uncertainty in the inputs $\mathbf{u}$.

2.1. The moving horizon estimator

The moving horizon estimator (MHE) is used in several forecast schemes to estimate the states and parameters of the dynamic iceberg model. The MHE is an optimization problem where the arrival cost term, process and measurement noises are minimized. The arrival costs summarizes the information available about the process, which is not included into the moving horizon, the measurement noise represents the uncertainty in the measurements of the iceberg position and the process noise is correlated to the error in the dynamic iceberg model (1), for instance uncertainties in the ocean current input. The MHE can be defined as follows (Robertson et al., 1996):

$$\min_{\{\mathbf{x}_k, \mathbf{w}_k, \mathbf{v}_k\}} \|\hat{\mathbf{x}}_M - \mathbf{x}_M\|^2_{\mathbf{P}^{-1}} + \sum_{k=M}^{\Gamma} \|\mathbf{v}_k\|^2_{\mathbf{R}^{-1}} + \sum_{k=M}^{\Gamma-1} \|\mathbf{w}_k\|^2_{\mathbf{Q}^{-1}} \tag{2a}$$

$$\begin{aligned} s.t. \quad & \mathbf{x}_{k+1} = \mathbf{f}(\mathbf{x}_k, \mathbf{u}_k) + \mathbf{w}_k \quad \forall k = M, ..., \Gamma - 1 \\ & \mathbf{y}_k = \mathbf{h}(\mathbf{x}_k) + \mathbf{v}_k \qquad \forall k = M, ..., \Gamma \\ & \mathbf{x}_k \in \mathbb{X}, \ \mathbf{w}_k \in \mathbb{W}, \ \mathbf{v}_k \in \mathbb{V}, \end{aligned} \tag{2b}$$

where $\hat{\mathbf{x}}$ is the estimated state, $\mathbf{P} \in \mathbb{R}^{n_x \times n_x}$ is the estimated error covariance matrix of the state estimate, $\mathbf{R} \in \mathbb{R}^{n_y \times n_y}$ the measurement noise covariance matrix and $\mathbf{Q} \in \mathbb{R}^{n_x \times n_x}$ the process noise covariance matrix. The matrix $\mathbf{Q}$ and $\mathbf{R}$ can be seen, in addition to their statistical interpretation, as a measure of confidence in the model equations and the process data, and hence be regarded as tuning parameters (Scibilia and Hovd, 2009). The horizon contains $(\Gamma - M + 1)$ measurements, taken at times $t_{k=M} < ... < t_{k=\Gamma}$. The measurement at t_Γ is the most recent iceberg position measurement, and the measurement at t_M represents the oldest measurement that is included in the horizon of the MHE.

The sets $\mathbb{X}$, $\mathbb{W}$ and $\mathbb{V}$ are closed and convex, and usually they are finite dimensional polyhedral sets

$$\begin{aligned} \mathbb{X} &= \{\mathbf{x}_k \in \mathbb{R}^{n_x} | \mathbf{D}_x \mathbf{x}_k \leq \mathbf{d}_x\}, \\ \mathbb{W} &= \{\mathbf{w}_k \in \mathbb{R}^{n_x} | \mathbf{D}_w \mathbf{w}_k \leq \mathbf{d}_w\}, \\ \mathbb{V} &= \{\mathbf{v}_k \in \mathbb{R}^{n_y} | \mathbf{D}_v \mathbf{v}_k \leq \mathbf{d}_v\}. \end{aligned} \tag{3}$$

The MHE formulation is a constrained non-linear least-squares problem. Optimization variables are $\mathbf{x}_k$, $\mathbf{w}_k$ and $\mathbf{v}_k$, which present the state, the process noise and the measurement noise vectors in the optimization horizon.

2.2. The extended Kalman Filter

In some of the forecast schemes the MHE can be replaced by the less complex extended Kalman filter (EKF). This may result in a loss of performance, but simplifies the implementation.

The EKF linearizes the non-linear system (1) around the last filter estimate and then applies the Kalman filter Rawlings and Bakshi (2006). With the following linearization

$$\mathbf{F}_k = \left.\frac{\partial \mathbf{f}_k}{\partial \mathbf{x}}\right|_{\hat{\mathbf{x}}_k^+}, \qquad \mathbf{H}_k = \left.\frac{\partial \mathbf{h}_k}{\partial \mathbf{x}}\right|_{\hat{\mathbf{x}}_k^-}, \tag{4}$$

the method can be summarized in a recursion with time update

$$\hat{\mathbf{x}}_{k+1}^- = \mathbf{f}(\hat{\mathbf{x}}_k^+, \mathbf{u}_k), \tag{5a}$$

$$\mathbf{P}_{k+1}^- = \mathbf{F}_k \mathbf{P}_k^+ \mathbf{F}_k^T + \mathbf{Q}, \tag{5b}$$

where the minus sign represents the a priori time update and the plus sign the a posteriori measurement update. In

a second step, the measurement update is performed and the mean and covariance are given by

$$\mathbf{K}_k = \mathbf{P}_k^- \mathbf{H}_k^T \left(\mathbf{H}_k \mathbf{P}_k^- \mathbf{H}_k^T + \mathbf{R} \right)^{-1}, \tag{6a}$$

$$\hat{\mathbf{x}}_k^+ = \hat{\mathbf{x}}_k^- + \mathbf{K}_k \left[\mathbf{y}_k - \mathbf{h}(\hat{\mathbf{x}}_k^-) \right] \tag{6b}$$

$$\mathbf{P}_k^+ = (\mathbf{I} - \mathbf{K}_k \mathbf{H}_k)\, \mathbf{P}_k^-, \tag{6c}$$

where $\mathbf{Q}$ and $\mathbf{R}$ are again the process and measurement noise covariances.

2.3. Vector-Autoregression model fitting

As an alternative to the momentum balance described in (1), we also study a vector-autoregression model (VAR) with the following structure

$$\mathbf{z}_k = \sum_{i=1}^{p} \mathbf{A}_i \mathbf{z}_{k-i} + \boldsymbol{\varepsilon}_k, \tag{7}$$

where p is the model order, $\mathbf{A}_i \in \mathbb{R}^{n_z \times n_z}$ are real-valued matrices containing the regression coefficients and $\boldsymbol{\varepsilon}_k \in \mathbb{R}^{n_z}$ is the residual, which is independently and identically distributed and serially uncorrelated (Barnett and Seth, 2014). The first represents the predictable structure of the data and the later the unpredictable. In context of this paper, $\mathbf{z} \in \mathbb{R}^{n_z}$ is either the two-dimensional iceberg velocity vector or a four-dimensional iceberg and wind velocity vector. The model (7) can be transformed into (1). The parameters of the VAR model (7), the coefficients $\mathbf{A}_i$ and the residual covariance matrix $\boldsymbol{\Sigma} = cov(\boldsymbol{\varepsilon}_k)$, are fitted to data by solving an optimization problem.

2.4. The multivariate empirical model decomposition

The multivariate empirical mode decomposition (MEMD) is a fully data-driven adaptive signal processing method. The MEMD is an extension to multivariate signals of the empirical model decomposition (EMD). The EMD decomposes a signal $\mathbf{z}(t)$ into amplitude- or frequency modulated components called intrinsic mode functions (IMFs) $\mathbf{c}_l(t)$ and a bias term $\mathbf{r}(t)$, such that

$$\mathbf{z}(t) = \sum_{l=1}^{T} \mathbf{c}_l(t) + \mathbf{r}(t), \tag{8}$$

where T is the amount of IMFs. An iterative process that extracts high frequency modes from slower ones extracts the IMFs (Aftab et al., 2016). An appealing property of the MEMD is its mode alignment that aligns "common scales", which are present in the multivariate data, in the same indexed IMFs (Ur Rehman and Mandic, 2010). In the context of this article $\mathbf{z}$ represents the iceberg velocity.

3. Iceberg Drift Forecast Schemes

In this section the iceberg drift forecast schemes are briefly introduced. The forecast schemes are categorized in kinematic, statistical and hybrid forecast schemes similar to those in Marko et al. (1988), and help to connect the forecast schemes presented here to previously published ideas.

The *dynamic* forecast model uses the momentum equation, which calculates the acceleration based on the sum of foreces acting on the iceberg. The *kinematic* forecast schemes predict the iceberg drift from superposition of past motions of the iceberg. The *statistical* forecast schemes use not only the observed iceberg motion, but also historical data at the iceberg location. A statistical iceberg model is fitted to the data that has a predictable and unpredictable part. The *hybrid* forecast schemes use a dynamic iceberg drift model but correct one or several parameters with help of the observed iceberg trajectory.

In the following sections it is explained how the forecasts are performed. In order to keep this review brief the particular methods that are used in a forecast scheme, like the moving horizon estimator or the empirical mode decomposition, are not explained in detail. Instead, a reference to the original paper and further references, directly explaining the particular methods used, are given in each section. Tab. 1 at the end of the section summarizes the performance of the methods.

3.1. Dynamic Forecast scheme

The dynamic forecast scheme (DYM) uses a dynamic iceberg drift model to predict the future iceberg trajectory (Eik, 2009). It is based on a momentum equation

$$m\mathbf{a} = \mathbf{f}_a + \mathbf{f}_c + \mathbf{f}_p + \mathbf{f}_{cor}, \tag{9}$$

where $\mathbf{a}$ is the iceberg acceleration and $\mathbf{f}_a$, $\mathbf{f}_c$, $\mathbf{f}_p$ and $\mathbf{f}_{cor}$ are the air drag, the water drag, the pressure gradient and Coriolis force, respectively. The total mass m of the iceberg consists of physical iceberg mass m_0 and added mass m_{add} ($m = m_0 + m_{add}$) due to the iceberg surrounding water field (Sodhi and El-Tahan, 1980). The mass and cross-sectional areas are calculated with the characteristic length L and width W of the iceberg

$$m = L_0 W_0 C_f (H_w + H_a) \rho_{Ice}, \tag{10}$$

where H_w and H_a are the keel depth and sail height, respectively. The shape factor C_f for different iceberg shapes can be found in McClintock et al. (2002). Other parameters like the air drag, water drag and added mass coefficients as well as water, air and ice densities are taken from Eik (2009).

3.2. Statistical Forecast scheme

3.2.1. The VAR model forecast scheme

The Vector-Autoregression (VAR) model forecast scheme was presented in Andersson et al. (2018). It uses the established kinematic relationship between iceberg, current and wind velocities

$$\boldsymbol{\nu} = \boldsymbol{\mu} + \alpha\boldsymbol{\omega}, \tag{11}$$

where $\boldsymbol{\nu}$, $\boldsymbol{\mu}$ and $\boldsymbol{\omega}$ are the iceberg, ocean current and wind velocity. The parameter α is about 0.017 to 0.02 (Smith, 1993; Garrett et al., 1985; Bigg et al., 1997; Wagner et al., 2017). In addition, a current VAR model is identified based on historical ocean current data in the region of interest. It is possible to identify a ocean current model for each grid cell for which current data is available, but it is also possible to choose one representative ocean current model for a certain region. The basic premise of the forecast scheme is that (11) holds and the current velocity (speed and direction) accounts for most of the uncertainty in the iceberg drift. The wind velocity, on the other hand, has a minor contribution to the uncertainty, since it is well forecasted by a weather forecast model. In this case the problem of forecasting the iceberg velocity can be transformed to a problem of forecasting the current velocity.

If wind information is received from a weather model, the following steps are performed in every forecast step for the VAR model:

1. Use a filter or estimator and the kinematic model (11) to obtain an estimate of the current velocity $\boldsymbol{\mu}$.
2. Forecast the current velocity $\boldsymbol{\mu}$ using the identified VAR ocean current model.
3. Use (11) and the forecasted current velocity $\boldsymbol{\mu}$ to calculate the corresponding iceberg velocity $\boldsymbol{\nu}$
4. Integrate to the iceberg position.

In the VAR forecast scheme only a value for α has to be chosen. This reduces considerably the amount of parameters in comparison to the forecast schemes that use the mechanistic dynamic iceberg model. Moreover, information about the iceberg geometry are not necessary and the double integration from acceleration to position is avoided. On the other hand, the training set that is used to identify the VAR ocean current model influences the forecast performance.

The complexity of the forecast produced with the VAR model is moderate, since the VAR model is linear and a simple filter, for instance the moving average filter, can be used to smooth the iceberg position measurements.

3.3. Kinematic Forecast schemes

3.3.1. The constant velocity forecast scheme

This is the simplest forecast model possible. It assumes that the iceberg velocity stays constant during the forecast periods and uses a simple integrator to calculate the iceberg position. Depending on the frequency in which iceberg position updates are available a filter is necessary to reduce the influence of measurement noise and fast frequency components. This forecast scheme is very simple and easy to implement, and provides a first estimate of the forecasted iceberg trajectory. Moreover, it is related to the theoretical current forecast scheme introduced below. Both schemes assume either constant iceberg velocity or constant current velocity, which has a similar effect in the water drag force.

3.3.2. The MEMD forecast scheme

The multivariate empirical mode decomposition (MEMD) forecast scheme was presented in Andersson et al. (2017a). It can detect oscillations, such as inertial or tidal oscillations, in the iceberg velocity signal. Several sources (ocean and weather models) that forecast current and wind velocities may be included to the scheme. These environmental models may forecast for a different time horizon and in different frequencies (daily, hourly etc.). Consequently, they may be more precise for different frequency bands.

The main idea is, therefore, to decompose the inputs (current and wind velocities) and the output (iceberg velocity) into frequency modulated components. Afterward, each frequency band is forecasted separately for each direction with the kinematic relationship

$$\boldsymbol{\nu}^i = \sum_k \eta_k^i \boldsymbol{\mu}_k^i + \sum_k \gamma_k^i \boldsymbol{\omega}_k^i, \tag{12}$$

where η and γ are weighting parameters. The superscripts are related to the frequency bands and the subscript to possible multiple inputs from different wind and ocean current models.

The model (12) is similar to the kinematic model (11), but also uses a weighting factor for the ocean current input. Smith (1993) used the same kinematic model, but he did not decompose the signal into different frequency bands. For each forecast step and frequency band the weighting parameters are recalculated based on the observed iceberg trajectory. Then it is evaluated for each frequency band based on the past observation of the iceberg trajectory whether the kinematic model (12) or a auto-regression model of the iceberg velocity is better to forecast the iceberg velocity. Consequently, prior to each forecast it is assessed if causality between inputs and outputs exists, which is known as the Granger's causality principle (Granger, 1969).

The decomposition of the input and output signals into their frequency bands is performed by the MEMD. Each frequency band is forecasted separately. Consequently, it is possible to include several wind and ocean current models, and choose for each frequency band which of them fit best to the observed iceberg velocity. On the other hand, this forecast scheme is the most complex and time consuming of all schemes presented in this article. In addition, it is necessary to observe the iceberg for some time. It is recommended to have at least two extrema of the oscillation that one would like to detect in the data set. In case of the iceberg drift the inertial and tidal oscillations are the most important fast oscillations. Therefore, the MEMD needs iceberg drift data of about one day before it can detect these oscillations. The measurement frequency should exceed the Nyquist frequency (about 6 h). The MEMD becomes more precise as more data becomes available. As the MEMD forecast is purely data driven it can be difficult to pinpoint the cause of a good or bad forecast result (Andersson et al., 2017a).

3.4. Hybrid forecast schemes

3.4.1. Ancillary current forecast scheme

The ancillary current forecast scheme (ACF) was proposed in Andersson et al. (2016a). It was also used in a switching scheme in Andersson et al. (2016c). The forecast scheme is a *hybrid* between mechanistic dynamic and statistical models, since it uses the mechanistic dynamic model but corrects some of its parameters based on the observed drift of the iceberg.

This forecast scheme was motivated by the idea of Smith (1993) who proposed to correct the drag coefficients (from air and water) of the dynamic iceberg model to improve the forecast. The correction of the drag coefficients based on past observation was also performed by Turnbull et al. (2015). In (Andersson et al., 2016a) it was shown if the drag coefficients are used as optimization variables the resulting variables lose their physical meaning and cannot be considered drag coefficients anymore. In addition, the estimated drag coefficient and chosen cross-sectional areas of the iceberg are codependent. If this correction scheme is used in a moving horizon window, strong changes and peaks of the drag coefficients were observed that degrade the forecast performance (Andersson et al., 2016a). The product of cross-sectional area and drag coefficients can only be estimated with a sufficiently long observation horizon (which guarantees that ocean current and wind inputs are unbiased).

Alternatively to correcting the drag coefficients, the idea of an ancillary current was proposed (Andersson et al., 2016a). The ancillary current is an artificial corrective current, which is added to the current input received from an ocean model

$$\tilde{\boldsymbol{\mu}} = \boldsymbol{\mu} + \boldsymbol{\mu}^*, \tag{13}$$

where $\boldsymbol{\mu}$, $\tilde{\boldsymbol{\mu}}$ and $\boldsymbol{\mu}^*$ are the current from the ocean model, the corrected current and the ancillary current, respectively. The ancillary current is assumed to be constant during the forecast and recalculated every time a new iceberg position measurement becomes available. This is done with a moving horizon estimator (Sec. 2.1). A simpler estimator, like the extended Kalman filter (Sec. 2.2), may also be used. The ancillary current has a smoother progression than the drag coefficients with less sudden changes and, therefore, improves the forecast performance considerably (Andersson et al., 2016a).

The underlying assumption of the ancillary current $\boldsymbol{\mu}^*$ is that the current from an ocean model $\boldsymbol{\mu}$ is biased, and that this bias changes only slowly over time. In fact, two other variables to correct the current input may also be used, e.g. absolute current velocity and direction. The desired property of the correction variables is that they only change slowly during the forecast.

In Andersson et al. (2016c) gives an example of how to predict the forecast performance based on the assumption that the ancillary current changes slowly over the forecast horizon.

3.4.2. Theoretical current forecast scheme

The ancillary current forecast scheme uses currents from an ocean model (or other sources) at all times. With the ancillary current the deficiencies of the iceberg drift model and the data are captured and corrected. The approach corrects the current input, since this input is the source of the largest uncertainty (error). During the short-term forecast the ancillary current is assumed constant, since it is assumed that the bias in the current input varies slowly. Consequently, it is assumed that the first derivative of the current input $\dot{\boldsymbol{\mu}}$ is approximately correct. If this is not the case and the ancillary current changes quickly, it may produce large forecast errors.

If the ancillary current changes quickly it may be beneficial to not use the current input $\boldsymbol{\mu}$ at all, but estimate the total theoretical current instead (Andersson et al., 2016c)

$$\hat{\boldsymbol{\mu}} = 0\boldsymbol{\mu} + \boldsymbol{\mu}^*, \tag{14}$$

where the $\mathbf{0}$ indicates that the ocean current input is not used.

The theoretical current $\hat{\boldsymbol{\mu}}$ and it is assumed constant during the forecast. The theoretical current can be estimated in the same way as the ancillary current.

The theoretical current forecast scheme (TCF) is strongly related to the ancillary forecast scheme, but avoids error propagation from the ocean current model (or other current sources). On the other hand, a possibly valuable source of information is excluded from the forecast scheme. In this forecast scheme the main changes in the iceberg velocity after the transition period are caused by wind and wave inputs. Consequently, this forecast scheme has similarities with the constant iceberg velocity forecast scheme, which is a much simpler forecast scheme (Sec. 3.3.1).

3.4.3. Inertial current forecast scheme

The inertial current forecast scheme (ICF) was presented in Andersson et al. (2016b).

The inertial current forecast scheme uses the mechanistic dynamic iceberg model in combination with a simple ocean current model. Instead of using a current input from ocean models or other sources as the ancillary current forecast scheme does, the inertial current forecast scheme estimates the complete ocean current. It assumes that the current consists of an oscillatory and slowly varying component

$$\tilde{\boldsymbol{\mu}} = \overline{\boldsymbol{\mu}} + \underline{\boldsymbol{\mu}}, \tag{15}$$

where $\overline{\boldsymbol{\mu}}$ and $\underline{\boldsymbol{\mu}}$ are the velocities of a inertial oscillation and slowly varying part, respectively.

The oscillatory part is the wind driven inertial oscillation, which can be approximated by

$$\dot{\overline{\boldsymbol{\mu}}} = \mathbf{B}(\boldsymbol{\omega}) + f\mathbf{k} \times \overline{\boldsymbol{\mu}} - c\overline{\boldsymbol{\mu}}, \tag{16}$$

where $\mathbf{B}(\boldsymbol{\omega})$ is the wind excitation, c is a decay factor, f is the Coriolis frequency and $\mathbf{k}$ is the unit vector directed upwards parallel to the z-axis (De Young and Tang, 1990).

Table 1: Brief summary of the forecast methods presented in Section 3. For each forecast method the name, abbreviation, classification, requirements and a short description is given. Except of the dynamic model every forecast scheme needs iceberg position measurements.

Name (-forecast scheme)	Abbr.	Classification	Requirement	Description
Dynamic model	DYM	dynamic	Current, wind, (waves) from meteorological and oceanographic models	Forecast of iceberg trajectory with momentum balance that calculates the acceleration based on sum of forces on the iceberg.
VAR model	VAR	statistical	Iceberg position meas.; Wind from meteorological model; Historical ocean current data	Offline identification of an statistical ocean current model. Estimation of iceberg and current velocity with kinematic iceberg model and a filter. The current velocity is forecasted with a statistical ocean current model, and the iceberg velocity is again calculated with kinematic iceberg model.
Constant velocity	CVF	kinematic	Iceberg position meas.	Estimation of iceberg velocity with filter. Constant iceberg velocity in forecast period.
MEMD model	MEMD	kinematic	Iceberg position meas.; Current, wind, (waves) from meteorological and oceanographic models (can be several)	Decomposition of inputs (current and wind vel.) and output (iceberg vel.) into frequency bands. Decision if causality exists between inputs and output for each frequency band. As a result iceberg vel. is forecasted in each band by linear combination of inputs or otherwise by autoregression.
Ancillary current	ACF	hybrid	Iceberg position meas.; Current, wind, (waves) from meteorological and oceanographic models	Correction of ocean current input of the dyn. model with estimated ancillary current, which is assumed constant during the forecast period.
Theoretical current	TCF	hybrid	Iceberg position meas.; Wind from meteorological model	Estimation of complete (theoretical) ocean current needed to explain observed iceberg drift. Does not use current input from ocean model. Estimated current is assumed constant in forecast period.
Inertial current	ICF	hybrid	Iceberg position meas.; Wind from meteorological model	Estimation of ocean current with simplified inertial and mean ocean current model. Mean current is assumed constant and oscillation of inertial current is propagated by a model in forecast period.

In the regions studied in this article the inertial oscillation has a period of about 12 h to 16 h.

The inertial current forecast scheme is more advanced than the theoretical current forecast scheme due to an explicit ocean current model. In this study the tidal currents were neglected in the inertial current forecast scheme. However, it is possible to extend (15) to explicitly consider the tidal currents, which should improve the method.

During the forecast the slowly varying part of the current is assumed constant while the oscillatory part is propagated with the model (16). Consequently, the inertial current forecast scheme is "located" between the ancillary and theoretical forecast schemes. Due to the explicit consideration of the inertial current it is expected that the slowly varying part is estimated more accurately. The estimation is challenging and performed with a moving horizon estimator (Andersson et al., 2016b). It is recommended to not use a simpler estimator, like the EKF, since it may have problems to separate the two current components.

4. Data Set

To assess the performance of the models described above, we compared their predictions with iceberg, current and wind data sets were recorded in 2015 and 2016. The characteristics of these data sets are described in detail below.

4.1. Iceberg Data

Two iceberg data sets are used for the comparison; one set of icebergs were tracked close to Newfoundland in Spring 2015, the other set was tracked in northern Baffin Bay in late summer 2016.

4.1.1. The Newfoundland data set

The GPS trackers on the icebergs close to Newfoundland were deployed by helicopter from the CCGS *Amundsen* during the Offshore Newfoundland Research Expedition on April 22th and 24th 2015. On Iceberg 1 and Iceberg 2 a Canatec GPS tracker was deployed. On Iceberg 4 two Canatec and two Solara GPS trackers were deployed. The beacons provided (at least) an hourly position update. For approximately the first 48 h after deployment the measurement frequency was considerably higher (five minutes frequency).

A summary of the Newfoundland iceberg data set is given in Tab. 2. The horizontal dimensions were estimated on sight and the keel depth measured with a ship-mounted SX90 sonar.

Iceberg 4 broke into two pieces after about 5.5 days. Thereafter, two icebergs, Iceberg 4 and Iceberg 4-3[1], were tracked. Considering the dimensions of Iceberg 2 it is likely that the iceberg rolled at the end of the tracking.

Iceberg 1 and Iceberg 2 drifted in close proximity to each other, but had very different drift trajectories. The same can be observed for Iceberg 4 and Iceberg 4-3 after their separation. The iceberg drift trajectories are shown in Fig. 2.

4.1.2. Baffin Bay data set

The GPS trackers on the icebergs in northern Baffin Bay were deployed by helicopter from the CCGS *Amundsen* in August 2016. The data set used here is within the period August to October 2016. The icebergs are named after

[1]The second number represents the GPS tracker.

(a) Iceberg 1 on April 22, 2015 - Shape: Dry dock.

(b) Iceberg 2 on April 22, 2015 - Shape: Rounded.

(c) Iceberg 4 on April 24, 2015 - Shape: Wedged

Figure 1: (a) Iceberg 1 located close to Bonavista on Newfoundland with horizontal dimensions of about 210×150 m. (b) Iceberg 2 located close to Bonavista on Newfoundland with horizontal dimensions of about 100×100 m. (c) Iceberg 4 with the horizontal dimensions of about 290×100 m.

Table 2: Newfoundland iceberg data set. The iceberg geometries are from the day of the GPS beacon deployment.

	Iceberg shape	**horizontal dimensions** [m]	**freeboard** [m]	**keel depth** [m]	**measurement frequency** [h]	**drift data** [days]	**GPS tracker**
Iceberg 1	dry-dock	210 × 150	30	45 – 60	1	8	Canatec
Iceberg 2	rounded	100 × 100	16	75	1	4	Canatec
Iceberg 4	wedged	290 × 100	30	90 – 100	1	37	2 Canatec & 2 (1) Solara
Iceberg 4-3	–	–	–	–	1	52	Solara

the GPS tracker serial number. The ice thicknesses were measured near the center of the icebergs with a 10 MHz ground-penetrating radar system, while the freeboards were estimated on sight (Tab. 3).

Iceberg 1040 was tracked with a MetOcean CALIB GPS beacon that was deployed on August 9, 2016 (Fig. 3a). The analysis performed here begins on August 17, 2016. However, due to a transmission error the same position measurement was received every three consecutive hours, reducing the effective sampling frequency for this iceberg to 3 h. The iceberg moved continuously in open water during the observation period. However, due to another data receiving error about two weeks of data was lost. Therefore, the iceberg trajectory is divided into two parts Iceberg 1040-1 and Iceberg 1040-2. The first part is from August 17 to September 22, 2016 and the second part from October 4 to 19, 2016.

Iceberg 5450 was tracked with a MetOcean CALIB GPS beacon that was deployed on August 9, 2016 (Fig. 3b). The analysis performed here begins on August 12, 2016. The iceberg grounded on August 21, 2016. The GEBCO 2014 global grid at 30 arc-second intervals suggests a sea depth of about 100 m at the grounding location GEBCO (-).

Iceberg 3534 was tracked with a RockSTAR^{TM} GPS receiver that was deployed on August 6, 2016 (Fig. 3c). The analysis begins on August 8, 2016. The iceberg grounded on August 23, 2016. After the first grounding event the iceberg began to move again for a few days. These periods were excluded from the data set, since they are short and the iceberg drift may be influenced strongly by gouging. The GEBCO 2014 global grid at 30 arc-second intervals bathymetry map suggest a sea depth at the first grounding position of about 190 m and at the final location of about 105 m. It may be that the bathymetry map overestimates the sea depth at the first "grounding event".

Iceberg 3651 was tracked with a RockSTAR^{TM} GPS receiver that was deployed on August 6, 2016 (Fig. 3d). The analysis begins on August 8, 2016. The iceberg grounded on August 19, 2016. The GEBCO 2014 global grid at 30 arc-second intervals suggests a sea depth of about 100 m at the grounding location GEBCO (-).

The iceberg drift trajectories are shown in Fig. 4.

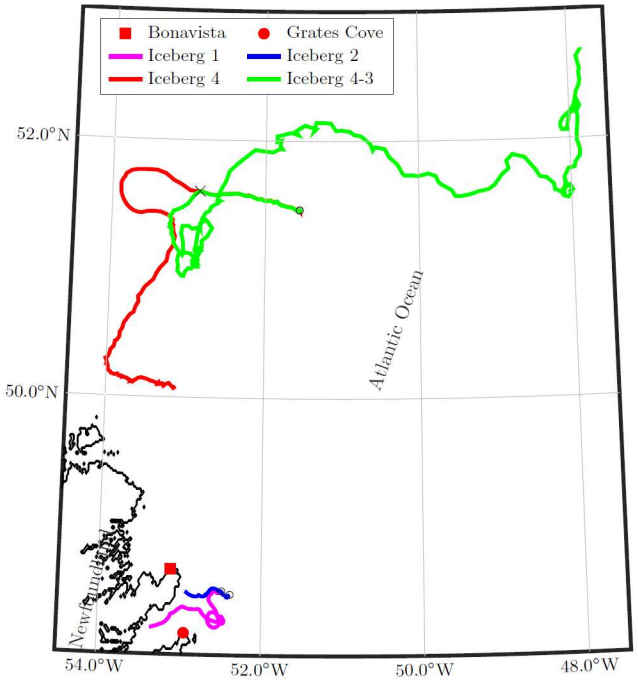

Figure 2: Map of iceberg drift trajectories. Iceberg 1 and Iceberg 2 are close to the shoreline of Newfoundland while Iceberg 4 and Iceberg 4-3 drift on the open ocean. The initial positions of the icebergs are marked with a circle and the location where the Iceberg 4 broke with a cross. For better orientation the weather stations in Bonavista and Grates Cove are marked on the map.

Table 3: Baffin Bay iceberg data set. The iceberg geometries are from the day of the GPS beacon deployment.

	Iceberg shape	**horizontal dimensions** [m]	**ice thickness** [m]	**freeboard** [m]	**measurement frequency** [h]	**drift data** [days]	**GPS tracker**
Iceberg 1040-1	tabular	1000 × 1000	92	–	1	36	MetOcean CALIB
Iceberg 1040-2	–	–	–	–	1	15	MetOcean CALIB
Iceberg 5450	tabular	600 × 400	67	–	1	8	MetOcean CALIB
Iceberg 3534	tabular	250 × 200	–	45	1	15	RockSTAR^{TM}
Iceberg 3651	tabular	300 × 300	–	40	1	11	RockSTAR^{TM}

4.2. Current data

The current data set was received from the E.U. Copernicus Marine Service (EU Copernicus Marine, 2006). The *Global Ocean 1/12° Physical Analysis and Forecast model updated daily* was used. The Operational Mercator global ocean analysis and forecast system at 1/12° provides 10 days of 3D global ocean forecasts updated daily. More specifically in this article the one hour surface current and daily layered mean current data is used. The depth of the layered current data is about 110 m. In fact, the current is already corrected by observation. Consequently, the case study presents hindcasts results. However, observation data in Northern Baffin Bay may be limited, reducing the possibility to correct the ocean current forecast.

The data assimilation into the model includes for instance drift data from SVP drifting buoys and sea surface height measurements from GLOSS, BODC and other sources. For more information the reader is advised to visit the E.U. Copernicus Marine Service webpage (EU Copernicus Marine, 2006).

4.3. Wind Data

As wind source, the *Global ocean wind L4 near real time 6 hourly observations* wind model from the E.U. Copernicus Marine Services is used. The wind fields are estimated from scatterometer retrievals. They have a horizontal resolution of 0.25°×0.25° and are updated every 6 h. Possible empty data points were removed from the data set. In addition, the wind data points were linearly interpolated onto the current grid cells. For more information the reader is advised to visit the E.U. Copernicus Marine Service webpage (EU Copernicus Marine, 2006). The wind data set does not represent forecasted wind. However, this will not influence the overall results and conclusions of the study. In fact, the dynamic iceberg drift model is likely the largest beneficiary.

5. Performance Indices

In order the quantify the forecast performance at a specific time, the mean $\hat{\zeta}$ over all end position forecast errors ζ =

(a) Iceberg 1040 on August 9, 2016 - Shape: Tabular

(b) Iceberg 5450 on August 9, 2016 - Shape: Tabular.

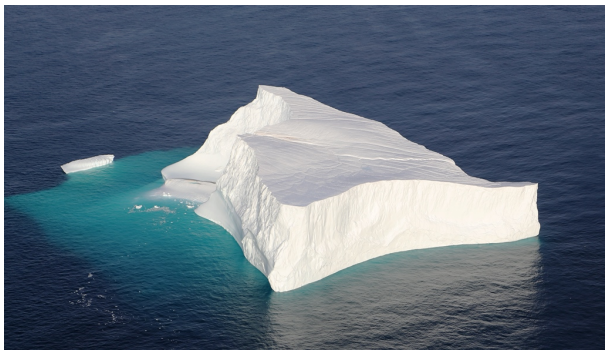

(c) Iceberg 3534 on August 6, 2016 - Shape: Tabular.

(d) Iceberg 3651 on August 6, 2016 - Shape: Tabular

Figure 3: (a) Iceberg 1040 located in northern Baffin Bay with horizontal dimensions of about 1000×1000 m and an ice thickness of 92 m. (b) Iceberg 5450 located in northern Baffin Bay with horizontal dimensions of about 600×400 m and an ice thickness of 67 m. (c) Iceberg 3534 located in northern Baffin Bay with horizontal dimensions of about 250×200 m and a freeboard of about 45 m. (d) Iceberg 3651 located in northern Baffin Bay with horizontal dimensions of about 300×300 m and a freeboard of about 40 m.

$|\hat{\boldsymbol{\chi}}_{k,end} - \boldsymbol{\chi}_{k,end}|$ is calculated

$$\hat{\zeta}_N = 1/K \sum_{k}^{K} \zeta_k, \tag{17}$$

where $\hat{\boldsymbol{\chi}}_{k,end}$ and $\boldsymbol{\chi}_{k,end}$ are the end position of the forecast and measured drift trajectory at time t_k, K is the amount of forecasts and N the length of the forecast period.

An alternative, which considers the whole forecasted trajectory and not just the end points, is the square root of the mean squared distance between the forecasted $\hat{\boldsymbol{\chi}}$ and measured $\boldsymbol{\chi}$ iceberg trajectory

$$\Xi_{N,k} = \sqrt{\frac{1}{N} \sum_{i=1}^{N} \|\hat{\boldsymbol{\chi}}(t_k + ih) - \boldsymbol{\chi}(t_k + ih)\|_2^2}, \tag{18}$$

where t_k is the initial time of the forecast and h is the time between measurements. The performance index (PI) for the whole observation horizon is the root mean square of ζ_N (18) with the same forecast horizon N

$$PI_N = \sqrt{\frac{1}{K} \sum_{i=k}^{K} \Xi_{N,k}^2}. \tag{19}$$

A relative performance index κ is the forecast error relative to the movement of the iceberg

$$\kappa = \frac{|\boldsymbol{\chi}_{k,end} - \hat{\boldsymbol{\chi}}_{k,end}|}{|\boldsymbol{\chi}_{k,end} - \boldsymbol{\chi}_{k,init}|}, \tag{20}$$

where $\boldsymbol{\chi}_{k,init}$ is the initial position of the measured iceberg trajectory at time t_k. For this article the following forecast categories for κ are chosen (Fig. 5):

- Bad forecast: $\kappa > 1$,
- Acceptable forecast: $1 \geq \kappa > 0.75$,
- Good forecast: $0.75 \geq \kappa > 0.5$,
- Excellent forecast: $\kappa < 0.5$.

6. Comparison Iceberg Drift Forecast

In this section the performance of the iceberg drift forecast methods are discussed. Each forecast method predicts every hour the iceberg trajectory. These forecasts are compared to the actual observed iceberg trajectory and the error is calculated (Section 5).

In addition to the short-term forecast schemes presented in Section 3, the static forecast scheme (STAT) is included in the comparison. It is a "pseudo" forecast, which assumes that the iceberg does not move but remains

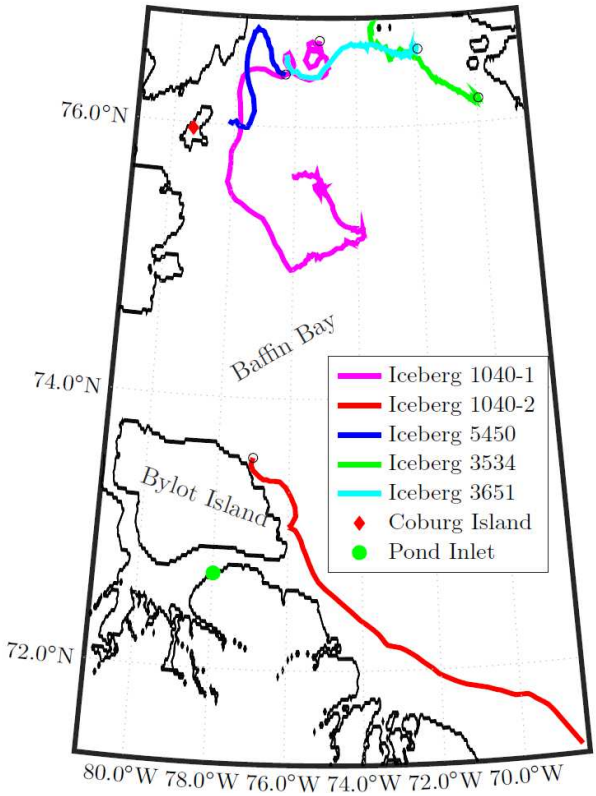

Figure 4: Map of iceberg drift trajectories. Iceberg 1040-1, 5450, 3534 and 3651 drift in the northern part of Baffin Bay. Iceberg 1040-2 drifts southwards towards Davis Strait. Bylot Island and two other land marks are shown on the map. The initial positions of the icebergs are marked with a circle.

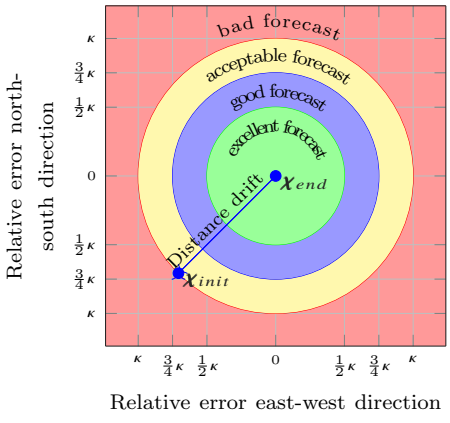

Figure 5: Relative performance index. If the end position of the iceberg forecast is encapsulated in the inner circle is defined as excellent, followed by two rings where the forecast is defined good and acceptable. If the forecast is not encapsulated by the outer circle is defined as bad.

at the initial location. It gives an indication of how fast the iceberg moves.

For each forecast method the same tuning was used for all iceberg trajectories to show the robustness of the methods. The amount of forecasts of each iceberg varies due to the varying amount of available data for each iceberg.

Since a longer period is examined, a simple deterioration model is implemented assuming a daily 2 % deterioration of the iceberg length, width, draft, and sail height. The results are relatively insensitive to different deterioration rates.

The discussion begins with Iceberg 2, since it is the iceberg with the shortest observation horizon, which helps to create clear figures. For the other icebergs it is often unpractical to show, for example, the forecast trajectories. A more detailed discussion of the forecast performance for the other icebergs is moved to the Appendix A.

6.1. Iceberg 2

For Iceberg 2 66 forecasts are performed. The mean end-position error (17) and the standard deviation of every forecast method for different forecast horizons are given in Tab. 4.

The MEMD forecast scheme performs best up to a forecast horizons of 12 h. However, the MEMD scheme needs more data than the other methods before a forecast can be performed. Therefore, it begins later than the others. For forecasts of 12 h to 18 h the TCF scheme performs best. The VAR forecast scheme produces the smallest error for a forecast horizon of 24 h. Interestingly, the standard deviation of CVF and STAT forecast scheme are small indicating that the iceberg velocity experience similar changes

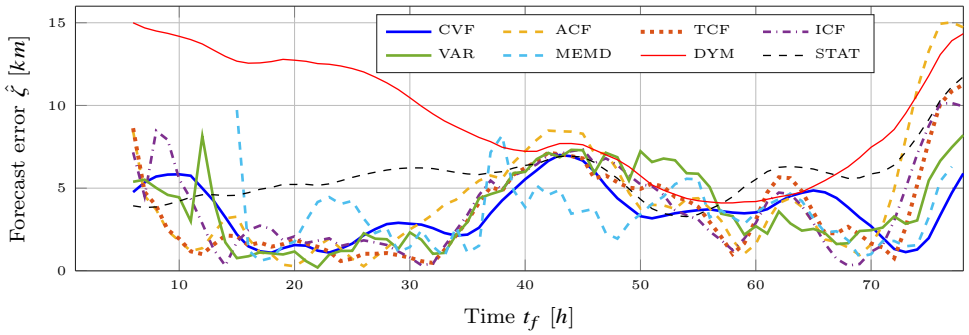

(a) Forecast error for different forecast schemes with a forecast horizon of 12 h for Iceberg 2.

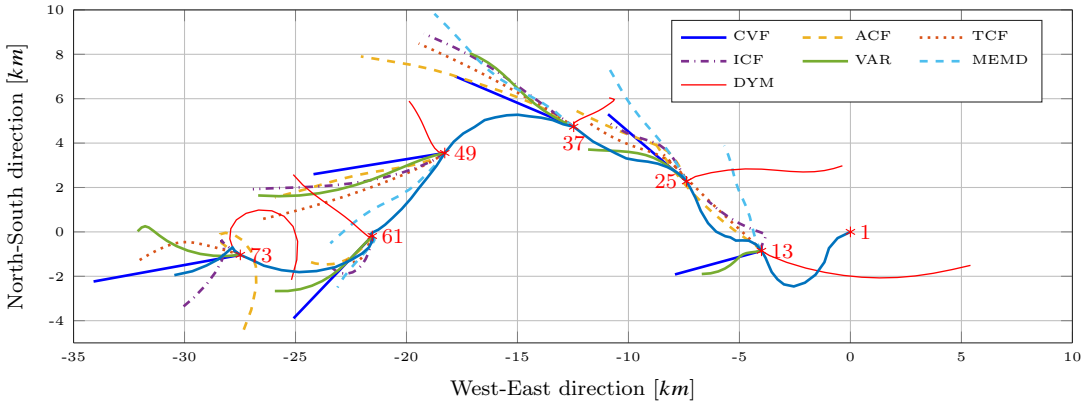

(b) Iceberg drift trajectory of Iceberg 2 and the 12 h forecast trajectories of the different forecast methods. The number marker corresponds to the time t_f in the upper figure.

Figure 6: Forecast results for Iceberg 2. The forecast error is shown in the upper figure, while the lower figure shows the corresponding iceberg drift trajectory.

over the whole observation horizon. The ancillary forecast scheme performs badly. One reason is that the ocean current input has to be corrected strongly. Moreover, this adaptation also changes constantly.

The end-position error of a 12 h forecast of every method is shown in Fig. 6a. The corresponding iceberg trajectory and the forecast trajectories of the different methods are shown in Fig. 6b. For reason of clarity the forecast trajectories are only shown for this iceberg and only every 12 h. Even though the forecast error is very similar for the statistical methods the end positions of the 12 h forecast trajectories differ considerably. Nevertheless, the forecast direction is often similar such that the trajectories are in the same sector.

The dynamic forecast model produces always a large forecast error, since the environmental forcing is not correctly represented for the iceberg. The ocean current direction is directed opposed to the drift direction over almost the entire observation period, which is the main reason for the large forecast error (mean absolute error about 140°). The wind direction correlates better with the iceberg drift in the observation horizon (mean absolute error about 60°), but at the beginning of the observation the iceberg drift and wind direction do not correlate well, which also contributes to the large forecast error in the first hours of the observation. Stronger winds and better directional correlation are the main reasons for the improvement of the dynamic iceberg forecast between 40 h to 65 h.

Table 4: Mean end-position-error (17) [km] for different forecast horizons of Iceberg 2. The standard deviation is given in brackets and the best forecast is marked bold. The best PI (19) is marked by a star. The static model gives an indication the iceberg drift distance within the forecast horizon.

	1 h	6 h	12 h	18 h	24 h
CVF	0.31 (0.18)	1.8 (1.0)	3.5 (1.7)	5.8* (2.5)	8.3* (3.4)
ACF	0.19 (0.10)	1.9 (1.3)	4.2 (3.5)	6.8 (4.1)	10.9 (5.8)
TCF	0.17 (0.08)	1.6 (1.0)	**3.6** (2.6)	**5.7** (3.5)	8.8 (5.1)
ICF	0.16 (0.07)	1.8 (0.9)	3.8 (2.6)	5.8 (3.7)	9.1 (5.1)
VAR	0.29 (0.16)	1.8 (0.9)	3.8 (2.3)	5.7 (3.7)	**8.0** (4.8)
MEMD	**0.10*** (0.05)	**1.6*** (0.8)	3.6* (1.7)	6.2 (3.0)	10.0 (6.2)
DYM	0.52 (0.22)	4.4 (1.9)	9.0 (3.6)	12.9 (5.4)	16.5 (6.6)
STAT	0.46 (0.18)	2.7 (1.0)	5.6 (1.7)	7.8 (1.4)	10.7 (2.3)

All statistical methods reduce the forecast error compared to the dynamic iceberg model considerably. The statistical models produce larger errors when the iceberg changes direction at 10 h and 45 h. The MEMD performs better than the other methods in the period 40 h to 50 h. Otherwise, it can be observed that the statistical methods behave similarly (Fig. 6a). Only the dynamic model has a completely different forecast behavior, because the badly specified environmental forces are not corrected.

Table 5: Mean end-position-error (17) [km] for different forecast horizons of Iceberg 1. The standard deviation is given in brackets and the best forecast is marked bold. The best PI (19) is marked by a star. The static model gives an indication the iceberg drift distance within the forecast horizon.

	1 h	6 h	12 h	18 h	24 h
CVF	0.81 (0.58)	5.2 (3.6)	9.6 (6.3)	15.0 (9.3)	20.6 (11.8)
ACF	0.34 (0.25)	**3.4*** (2.3)	7.3* (4.5)	11.8 (6.9)	17.5 (9.1)
TCF	0.38 (0.29)	4.0 (2.8)	8.6 (5.5)	13.0 (7.9)	18.6 (10.2)
ICF	0.33 (0.22)	3.6 (2.0)	7.8 (4.3)	12.0 (6.7)	17.1 (8.5)
VAR	0.72 (0.52)	3.9 (2.7)	**6.6** (4.2)	**9.6*** (6.1)	**12.8*** (7.5)
MEMD	**0.25*** (0.21)	4.0 (2.7)	8.5 (5.2)	14.3 (10.4)	22.3 (24.1)
DYM	0.70 (0.46)	5.0 (2.3)	9.5 (4.5)	13.7 (6.2)	17.6 (7.2)
STAT	0.87 (0.58)	4.9 (3.0)	8.5 (5.0)	11.5 (7.1)	14.4 (9.0)

Table 6: Mean end-position-error (17) [km] for different forecast horizons of Iceberg 4. The standard deviation is given in brackets and the best forecast is marked bold. The best PI (19) is marked by a star. The static model gives an indication the iceberg drift distance within the forecast horizon.

	1 h	6 h	12 h	18 h	24 h
CVF	0.35 (0.19)	1.9 (1.2)	3.5 (2.8)	5.7 (4.5)	8.1 (6.5)
ACF	0.22 (0.13)	2.2 (1.2)	4.2 (2.4)	6.7 (3.8)	9.6 (5.6)
TCF	0.21 (0.12)	2.0 (1.1)	3.9 (2.2)	6.2 (3.7)	9.0 (5.7)
ICF	0.18 (0.11)	**1.8*** (1.0)	3.6 (2.1)	5.8 (3.6)	8.4 (5.4)
VAR	0.33 (0.18)	**1.8** (1.0)	**3.0*** (2.2)	**4.8*** (3.6)	**7.1*** (5.2)
MEMD	**0.14*** (0.09)	2.1 (1.2)	4.1 (2.6)	6.7 (4.3)	9.7 (6.5)
DYM	0.38 (0.24)	3.4 (2.0)	7.2 (3.7)	11.1 (5.4)	14.7 (7.0)
STAT	0.68 (0.40)	4.0 (2.3)	7.7 (4.4)	11.5 (6.3)	15.2 (8.2)

Table 7: Mean end-position-error (17) [km] for different forecast horizons of Iceberg 4-3. The standard deviation is given in brackets and the best forecast is marked bold. The best PI (19) is marked by a star. The static model gives an indication the iceberg drift distance within the forecast horizon.

	1 h	6 h	12 h	18 h	24 h
CVF	0.74 (0.51)	4.6 (3.4)	8.2 (5.8)	12.9 (8.3)	17.9 (11.4)
ACF	0.31 (0.19)	3.3 (2.1)	6.5 (4.5)	9.3 (6.1)	13.3 (8.5)
TCF	0.33 (0.21)	3.6 (2.4)	7.2 (5.3)	10.0 (6.9)	14.4 (9.4)
ICF	0.26* (0.17)	**2.7*** (1.8)	**5.7*** (3.9)	8.2* (5.4)	11.5 (7.3)
VAR	0.66 (0.45)	3.6 (2.5)	5.7 (4.0)	**8.0** (5.1)	**10.5*** (6.7)
MEMD	**0.25*** (0.18)	4.0 (2.7)	7.9 (5.2)	11.65 (7.2)	15.9 (9.7)
DYM	0.65 (0.44)	3.7 (2.4)	6.7 (4.2)	9.58 (5.9)	12.5 (7.5)
STAT	0.99 (0.55)	5.6 (3.0)	10.3 (5.3)	14.70 (7.4)	18.9 (9.6)

Table 8: Mean end-position-error (17) [km] for different forecast horizons of Iceberg 1040-1. The standard deviation is given in brackets and the best forecast is marked bold. The best PI (19) is marked by a star. The static model gives an indication the iceberg drift distance within the forecast horizon.

	1 h	6 h	12 h	18 h	24 h
CVF	0.53 (0.33)	2.85 (2.0)	5.8 (4.6)	9.9 (7.5)	14.0 (10.5)
ACF	0.31 (0.27)	2.9 (1.8)	5.3 (3.5)	9.2 (6.4)	12.5 (9.3)
TCF	0.31 (0.27)	2.9 (1.9)	5.2 (3.9)	9.1 (6.9)	12.5 (10.1)
ICF	0.25 (0.24)	**2.3*** (1.5)	**4.7*** (3.5)	**8.2*** (6.5)	**11.7*** (9.6)
VAR	0.51 (0.31)	2.6 (1.8)	5.3 (4.0)	8.8 (6.9)	12.4 (9.8)
MEMD	**0.22*** (0.13)	3.3 (2.0)	6.1 (4.1)	10.9 (7.1)	15.5 (10.5)
DYM	0.57 (0.29)	3.7 (2.0)	7.1 (4.2)	10.6 (6.1)	13.5 (7.8)
STAT	0.80 (0.49)	4.4 (2.8)	8.0 (5.3)	11.7 (7.6)	14.8 (9.8)

6.2. Iceberg 1

For Iceberg 1 160 forecasts are performed. The mean end-position error (17) and the standard deviation of all methods are shown in Tab. 5. The considerable larger forecast errors compared to Iceberg 2 are caused by several loops with a period of about 18 h to 24 h in the iceberg trajectory that are most likely caused by the current flows in and out of Conception Bay (between Grates Cove and Bonavista (Fig. 2)). A more detailed discussion can be found in Appendix A.1.

6.3. Iceberg 4

For Iceberg 4 674 forecasts are performed. It breaks apart after about 5.5 days. After evaluating the pictures of the iceberg, it is assumed that breakage happens at about 2/3 of the waterline length. Mass, width, draft, and sail are adjusted accordingly in the simulations. The two remaining icebergs (Iceberg 4 and Iceberg 4-3) are likely more dome-shaped than wedged. The shape factor is, therefore, adjusted after the breakage.

The performance of each forecast method is given in Tab. 6. The forecast of Iceberg 4 is much better than of Iceberg 1. The dynamic forecast model is outperformed by all statistical methods for the considered forecast horizons. Large errors in the statistical forecast (besides the MEMD and CVF) are not observed. More details can be found in Appendix A.2.

6.4. Iceberg 4-3

For Iceberg 4-3 1161 forecasts are performed. The performance of each forecast method is given in Tab. 7. It is expected that the iceberg is small since it is a piece of Iceberg 4. The iceberg moves relative quick and the drift trajectory has several loops and direction changes. Therefore, the CVF and TCF that assume constant iceberg or current velocity perform not well. The introduction of the inertial current model in the ICF helps to detect the fast frequency components and improves the forecast considerably. Similarly the VAR model is able to forecast some of the fast frequency components if they are present in the training data set. Hence, the detection of fast frequency components and the ability to forecast them, improves the forecast compared to methods, like CVF, that are unable to do it. More details about Iceberg 4-3 can be found in Appendix A.3.

6.5. Iceberg 1040-1

For Iceberg 1040-1 865 forecasts are performed (Tab. 8). The ICF forecast scheme has the best forecast results since it is able to forecast fast frequency components. An additional advantage is that Iceberg 1040-1 is tracked in northern Baffin Bay where tidal and inertial frequencies are similar. The tidal current is not explicitly considered in the method, but it will correctly be detected and forecasted if it dominates the inertial current oscillation. More details about Iceberg 1040-1 can be found in Appendix A.4.

6.6. Iceberg 1040-2

For Iceberg 1040-2 865 forecasts are performed (Tab. 9). The absolute error only increases slightly compared to the

Table 9: Mean end-position-error (17) [km] for different forecast horizons of Iceberg 1040-2. The standard deviation is given in brackets and the best forecast is marked bold. The best PI (19) is marked by a star. The static model gives an indication the iceberg drift distance within the forecast horizon.

	1 h	6 h	12 h	18 h	24 h
CVF	0.34 (0.28)	2.4 (1.7)	5.8 (3.8)	9.7 (6.0)	13.7 (8.1)
ACF	0.21 (0.25)	2.4 (1.8)	6.4 (4.7)	11.4 (8.1)	16.5 (11.4)
TCF	0.19 (0.24)	**2.0*** (1.4)	**5.2*** (3.2)	**9.0*** (5.5)	**12.9*** (7.7)
ICF	0.20 (0.24)	2.1 (1.4)	5.3 (3.2)	9.1 (5.4)	13.1 (7.5)
VAR	0.31 (0.27)	2.3 (1.7)	5.8 (3.9)	9.6 (6.2)	13.5 (8.6)
MEMD	**0.14*** (0.14)	2.8 (2.0)	6.9 (4.3)	11.7 (7.5)	17.1 (12.0)
DYM	0.61 (0.55)	5.2 (4.8)	10.7 (9.8)	15.8 (14.5)	20.3 (18.7)
STAT	1.08 (0.50)	6.4 (2.8)	12.8 (5.3)	19.2 (7.7)	25.6 (9.7)

Table 10: Mean end-position-error (17) [km] for different forecast horizons of Iceberg 5450. The standard deviation is given in brackets and the best forecast is marked bold. The best PI (19) is marked by a star. The static model gives an indication the iceberg drift distance within the forecast horizon.

	1 h	6 h	12 h	18 h	24 h
CVF	0.38 (0.20)	2.0 (1.1)	4.2 (1.8)	7.4 (3.4)	11.1 (4.8)
ACF	0.20 (0.11)	2.1 (1.2)	3.7 (2.2)	6.5 (3.9)	9.5 (5.5)
TCF	0.20 (0.12)	2.1 (1.2)	3.7 (2.1)	6.6 (3.8)	9.7 (5.4)
ICF	0.17 (0.10)	**1.8*** (1.1)	3.7 (2.1)	6.7 (3.7)	10.0 (5.3)
VAR	0.37 (0.20)	2.0 (1.1)	**3.6*** (1.7)	**6.4*** (3.3)	**9.4*** (4.4)
MEMD	**0.15*** (0.08)	2.1 (1.2)	4.6 (2.0)	8.2 (4.0)	12.2 (5.9)
DYM	0.45 (0.25)	3.9 (1.6)	8.6 (2.6)	13.4 (3.9)	18.1 (4.8)
STAT	0.79 (0.40)	4.6 (2.1)	9.1 (3.7)	13.5 (5.4)	17.8 (6.9)

Table 11: Mean end-position-error (17) [km] for different forecast horizons of Iceberg 3534. The standard deviation is given in brackets and the best forecast is marked bold. The best PI (19) is marked by a star. The static model gives an indication the iceberg drift distance within the forecast horizon.

	1 h	6 h	12 h	18 h	24 h
CVF	0.42 (0.30)	2.0 (1.5)	3.1 (2.1)	5.2 (3.8)	6.9 (5.2)
ACF	0.29 (0.24)	2.7 (2.0)	3.3 (2.6)	5.9 (4.5)	7.0 (5.5)
TCF	0.29 (0.23)	2.6 (2.0)	3.2 (2.6)	5.7 (4.6)	6.8 (5.7)
ICF	**0.20*** (0.15)	**1.8*** (1.2)	2.4* (1.7)	4.2* (3.0)	**5.2** (4.0)
VAR	0.41 (0.29)	1.8 (1.3)	**2.3*** (1.7)	**4.0** (3.0)	5.4* (4.1)
MEMD	0.22 (0.16)	2.4 (1.8)	3.2 (2.2)	5.3 (3.0)	6.7 (5.0)
DYM	0.42 (0.30)	2.2 (1.6)	3.6 (2.3)	5.6 (3.7)	7.2 (4.5)
STAT	0.54 (0.39)	2.8 (2.0)	4.7 (3.1)	7.1 (4.6)	9.2 (5.7)

Table 12: Mean end-position-error (17) [km] for different forecast horizons of Iceberg 3651. The standard deviation is given in brackets and the best forecast is marked bold. The best PI (19) is marked by a star. The static model gives an indication the iceberg drift distance within the forecast horizon.

	1 h	6 h	12 h	18 h	24 h
CVF	0.42 (0.27)	2.1 (1.7)	3.3 (4.0)	6.0 (6.4)	8.3 (9.4)
ACF	0.24 (0.15)	2.5 (1.6)	4.0 (3.4)	7.1 (6.1)	9.5 (9.0)
TCF	0.24 (0.15)	2.4 (1.6)	3.7 (3.4)	6.6 (6.1)	8.8 (9.0)
ICF	**0.16*** (0.12)	**1.5*** (1.4)	3.0 (3.5)	5.4 (6.3)	7.9 (9.4)
VAR	0.40 (0.25)	1.9 (1.4)	**2.6*** (3.1)	**4.6*** (5.1)	**6.5*** (7.0)
MEMD	0.18 (0.10)	2.3 (1.8)	4.2 (4.0)	7.8 (8.7)	11.9 (18.8)
DYM	0.46 (0.31)	2.9 (2.1)	5.2 (4.5)	8.4 (6.5)	11.1 (8.4)
STAT	0.63 (0.42)	3.3 (2.4)	5.9 (4.8)	9.1 (7.0)	11.9 (9.0)

error of Iceberg 1040-1 even though the iceberg moves much faster as indicated by the static forecast error. The TCF performs best since the mean ocean current dominates the fast frequency components. Therefore, an explicit consideration of them in the ICF or VAR forecast scheme does not improve the forecast. More details about Iceberg 1040-2 can be found in Appendix Appendix A.5.

6.7. Iceberg 5450

For Iceberg 5450 173 forecasts are performed (Tab. 10). The mean error and standard deviation are similar for the statistical methods. More details about Iceberg 5450 can be found in Appendix A.6.

6.8. Iceberg 3534

For Iceberg 3534 334 forecasts are performed. The mean end-position error (17) for all forecasts is extremely small (Tab. 11). The VAR and ICF methods have a similar performance and outperform the other statistical methods. The iceberg moves relatively slowly, which explains the small absolute forecast error, which is the smallest of all icebergs discussed in this article. However, the standard deviation in comparison to drift forecast of the other icebergs is only superior for longer forecast horizons. More details can be found in Appendix A.7.

6.9. Iceberg 3651

For Iceberg 3651 250 forecasts are performed (Tab. 12). For shorter forecast horizons (1 h to 6 h) the ICF scheme performs best, while for longer forecast horizons (12 h to 24 h) the VAR scheme produces the best forecast. All statistical models outperform the dynamic model. However, the VAR model is by far the best for longer forecast horizons.

The forecast error for this iceberg is relatively small. Iceberg 3651 moves quicker than Iceberg 3534, which causes the larger absolute forecast error. The average velocity of Iceberg 3534 is 12 cm/s and of Iceberg 3651 it is 16 cm/s. More details can be found in Appendix A.8.

6.10. Summary of Iceberg forecasts

Fig. 7 displays the relative forecast performance of different methods of all icebergs. Even though the absolute error of Iceberg 3534 and Iceberg 3651 was smallest, Iceberg 1040-2 was forecasted the best relatively. Considering that the drift trajectory of Iceberg 1040-2 did not have loops or sudden direction changes, this is not surprising. The larger absolute error is caused by the considerable faster drift velocity.

Iceberg 1 was forecasted worse in relative and absolute values. The reason is the multiple loops in the observation period that are neither within the inertial nor tidal frequency.

Quantitatively, the difference between the performance indices (17) and (19) is relatively small and usually the same method performs best considering both indices. Therefore, the mean end position error (17) was usually used in this article, since the value is intuitive and easy to understand.

In comparison to the statistical methods it can be observed that in general the MEMD forecast scheme predicts

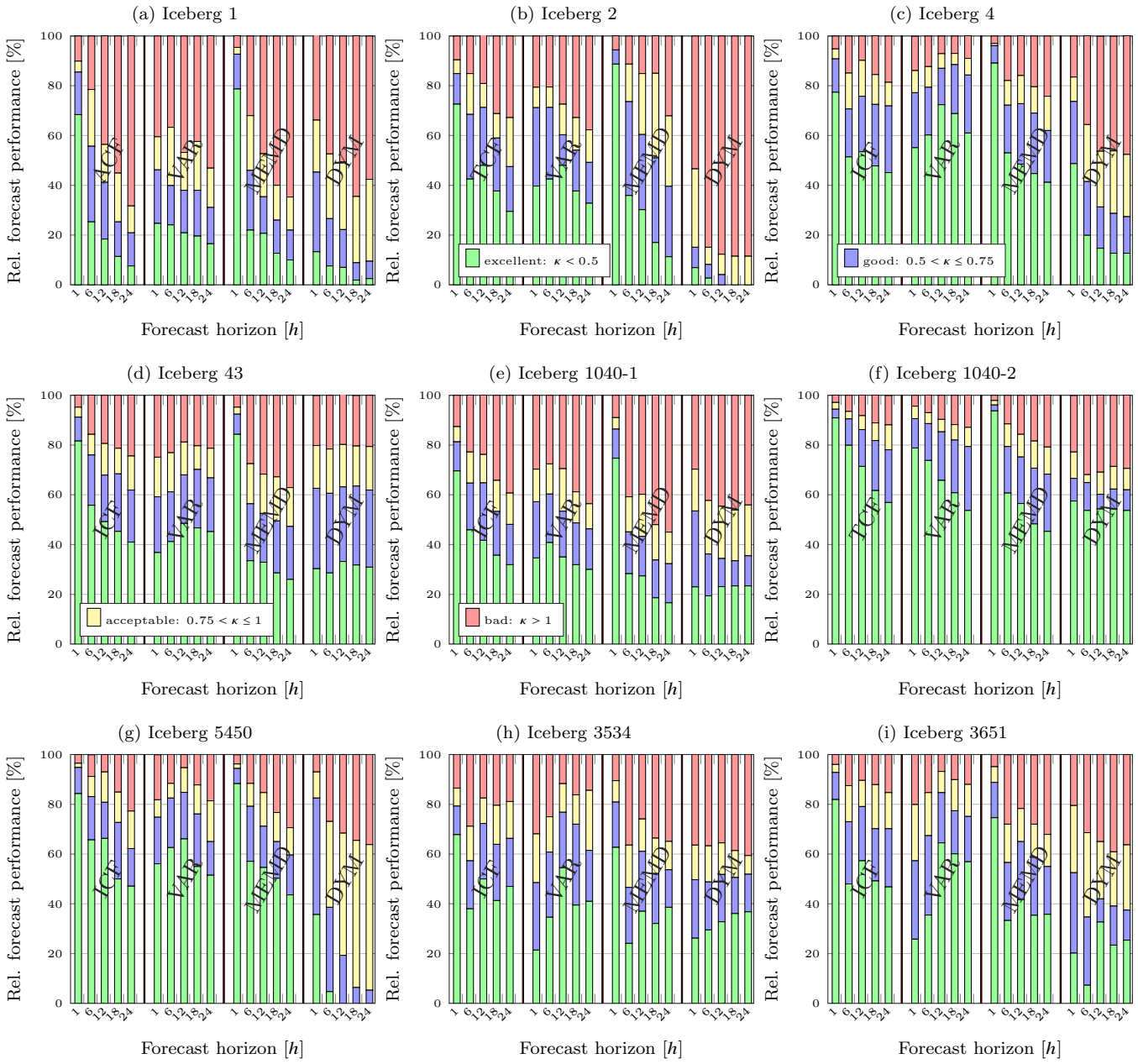

Figure 7: Relative forecast performance of the icebergs (subcaption above each figure). The relative forecast performance is grouped in four categories (Sec. 5): bad (red), acceptable (yellow), good (blue), excellent (green). Each iceberg forecast performed is grouped in one of the categories. Each vertical bar shows the percentage of each category for a certain method and forecast horizon. The best of ACF, TCF or ICF is on the left hand side, followed by the VAR model and MEMD model. The dynamic model is on the right-hand side.

the iceberg trajectory in the first hour very well. However, it degrades quickly for longer forecast horizons and produces a large absolute error. Considering the relative performance of the MEMD forecast scheme, which is only slightly worse than the VAR or ICF forecast schemes, one can see that the MEMD forecast scheme produces large forecasts error in cases when it produces a *bad* forecast. This is also indicated by a usually larger standard deviation of the MEMD forecast scheme.

The ICF or the VAR model usually produce the best statistical forecast. In fact, the ICF model is often better for shorter forecast horizons while the VAR model for longer. Therefore, a combination of both methods would be preferable.

For many of the iceberg trajectories it can be observed that the relative performance for the 12 h forecast is slightly better than the 6 h forecast. Most likely this is caused by the tidal current, which is either filtered or approximated. Its oscillation period correlates with the 12 h forecast. The largest offset is expected after 6 h. Moreover, it can be observed that the correct detection of the fast oscillations (inertial and tidal oscillations) improves the forecast, even

though the oscillations themselves have only a minor influence on the forecast (especially 12 h and 24 h). However, a correct detection of the oscillations influences how well the non-oscillating part of the ocean current is estimated. Since the non-oscillating part is often assumed to be constant (or only changes slightly) in the statistical forecast schemes, its correct estimation at the beginning of the forecast is important.

An improvement with the statistical models in comparison to the dynamic model can be observed for all trajectories. However, the relative performance usually decreases for longer forecast horizons more strongly for the statistical methods than for the dynamic model. Consequently, for even longer forecast horizons it is likely that the dynamic model at some point will produce a *less worse* forecast than the statistical methods. An interesting observation is that the standard deviation relative to the mean error is usually larger for the statistical methods than for the dynamic forecast method, even though both measures are smaller in absolute values for the statistical methods.

7. New statistical forecast schemes

The comparison of the statistical methods in the previous section revealed that the ICF and VAR forecast schemes performed overall the best. Moreover, it was determined that the ICF forecast scheme usually performs better for shorter periods while the VAR forecast scheme is usually better longer forecast horizons.

Two different ways of how to combine the two methods can be thought of:

1. Replacing the moving average filter in the VAR forecast scheme with a Kalman filter using the identified VAR model as the observer model (VAR KF).
2. Instead of using a constant current input in the ICF and TCF forecast scheme, the current may be forecasted with the VAR model forecast (ICF VAR and TCF VAR).

For the first approach the VAR model is transformed into a state space model. Since this model is linear a Kalman filter and not a MHE is used. The estimated of iceberg and ocean current velocity at the beginning of the forecast becomes so model based. This decreases the time delay in the velocity estimates, which was introduced when a simple moving average filter was used. Moreover, a more precise detecting of measurement and process noise is possible. On the other hand, the filtering becomes more aggressive, meaning the velocity is less smooth compared to the moving average filter (this depends also on the tuning of the Kalman filter).

The forecast results for this approach for the data sets used in this study are shown in Tab. 13. The forecast of Iceberg 1, 2, 1040-2 and 5450 improves. Moreover, the 6 h forecast of Iceberg 4 and 4-3 improves. However, not all forecasts can be improved. The forecast performance of Iceberg 4-3, 3534 and 3651 decreases quite a bit for longer forecast horizons (12 h to 24 h). For Iceberg 4-3 the new approach increases the errors slightly for each of the peaks in the forecast performance (Fig. A.10a). This may be reduced by a less aggressive filter with stronger smoothing. For Iceberg 3534 the overall performance for longer forecast horizons (12 h to 24 h)) is better with the VAR model. Again, this may be due to a stronger smoothing. A similar observation can be done for Iceberg 3651. In fact, the new approach reduces the large error at the end of the observation horizon but increases it slightly during the other periods (Fig. A.15a). In comparison to the VAR model forecast the 1 h and 6 h forecast of the new approach is clearly improved. It has to be kept in mind that the results depend on the tuning of the process and measurement covariances of the Kalman filter.

The inclusion of the VAR model forecast into the ICF forecast scheme is shown in Tab. 14. In general, it can be observed that the combination ICF and VAR is better than TCF and VAR. For some of the icebergs the 6 h forecast improves, however, a strong tendency to large outliers was observed. These have to be detected and removed from the forecast. A different tuning of the MHE may improve the situation. Nevertheless, it is not straight forward to improve the forecast performance by including the VAR forecast into the ICF forecast scheme.

8. Conclusion and Future Work

In this article different iceberg forecast schemes were compared over a forecast horizon of 1 h to 24 h. A summary of the average performance of every method on the presented iceberg tracks is given in Tab. 15. As expected the statistical forecast models generally outperformed the dynamic forecast model. However, it was also shown that the dynamic model sometimes performs better than the statistical methods. From the statistical forecast models the ICF and VAR model performed the best. On the other hand, each of the proposed statistical forecast models performed for specific icebergs and forecast horizons better than the others. The MEMD forecast scheme usually produced the best forecast for forecast horizons of about 1 h. The ICF forecast scheme performed well for forecast horizons up to 12 h, while the VAR forecast scheme usually performed best for longer forecast horizons (12 h to 24 h).

The MEMD and ACF forecast scheme generally do not perform well for longer forecast horizons (12 h to 24 h). In both cases the assumptions seemed to not hold. For the ACF it seems the assumption that the current model can be corrected with a constant term is not valid for longer forecast horizons. For the MEMD forecast scheme the assumption that all identified oscillations continue with a similar amplitude and frequency introduces a large error for longer forecast horizons (12 h to 24 h).

It has to be kept in mind, that the end-position errors (17) presented in this article can be influenced by tuning of the filters and estimators. We did not use an extensive amount of time on tuning. We also used the same tuning

Table 13: Mean end-position-error (17) [km] for different forecast horizons of VAR forecast scheme with the Kalman filter. The standard deviation is given in brackets and bold numbers show an improvement of the forecast in comparison to the previous proposed forecast schemes.

	1 h	6 h	12 h	18 h	24 h
Iceberg 1	0.28 (0.24)	**2.5** (1.9)	**6.1** (3.7)	**9.1** (5.5)	**12.6** (6.8)
Iceberg 2	0.14 (0.08)	**1.5** (0.7)	4.0 (2.0)	**4.9** (2.5)	**7.0** (3.4)
Iceberg 4	0.21 (0.12)	**1.7** (1.0)	3.3 (2.3)	4.9 (3.6)	7.2 (5.4)
Iceberg 4-3	0.28 (0.19)	**2.7** (1.8)	6.5 (4.4)	10.0 (6.6)	14.44 (9.2)
Iceberg 1040-1	0.40 (0.26)	2.4 (1.5)	4.9 (3.2)	8.3 (5.6)	12.0 (7.9)
Iceberg 1040-2	0.20 (0.24)	**1.9** (1.5)	**4.6** (3.1)	**7.7** (4.9)	**11.2** (6.8)
Iceberg 5450	0.27 (0.14)	1.9 (1.1)	**3.3** (1.9)	**5.9** (3.5)	**9.1** (4.6)
Iceberg 3534	0.37 (0.24)	2.0 (1.3)	2.7 (2.0)	4.8 (3.4)	6.1 (4.3)
Iceberg 3651	0.29 (0.18)	1.7 (1.1)	2.9 (2.6)	5.4 (4.8)	7.8 (7.0)

Table 14: Mean end-position-error (17) [km] for different forecast horizons of the ICF scheme forecasting the current with the VAR model. The standard deviation is given in brackets and bold numbers show an improvement of the forecast in comparison to the previous proposed forecast schemes.

	1 h	6 h	12 h	18 h	24 h
Iceberg 1	0.33 (0.22)	2.8 (1.8)	6.7 (4.8)	9.8 (6.6)	13.3 (8.3)
Iceberg 2	0.16 (0.07)	**1.5** (0.9)	3.9 (2.2)	**5.5** (3.3)	**7.9** (4.3)
Iceberg 4	0.18 (0.11)	**1.6** (0.9)	3.6 (2.3)	5.8 (3.7)	8.6 (5.5)
Iceberg 4-3	0.26 (0.17)	**2.5** (1.9)	6.5 (5.4)	9.3 (7.3)	13.2 (10.5)
Iceberg 1040-1	0.27 (0.24)	2.7 (1.9)	6.7 (5.5)	10.9 (8.7)	15.3 (12.6)
Iceberg 1040-2	0.20 (0.24)	2.3 (3.5)	6.5 (10.4)	10.6 (15.1)	15.04 (21.6)
Iceberg 5450	0.17 (0.10)	**1.7** (1.1)	3.7 (2.0)	6.5 (3.3)	9.8 (4.7)
Iceberg 3534	0.20 (0.15)	1.9 (1.4)	3.1 (2.8)	4.8 (4.3)	6.34 (5.8)
Iceberg 3651	0.16 (0.12)	**1.5** (1.3)	3.1 (3.2)	5.3 (5.5)	7.8 (8.0)

for all iceberg tracks. The results may be improved by improved tuning or individual tuning for each track. In general it can not be expected that a tuning that worked well on one track will also work well on another track, since the drift behavior of the icebergs is quite different. Sometimes a strong filtering of the iceberg velocity improves the forecast, even though it introduces a delay. In other cases the delay is the cause of a bad forecast. This two mechanism are the main difference between the VAR and VAR KF forecast method. It is difficult to tell a priori which tuning is better, but it was observed that strong filtering improves longer while aggressive filtering shorter forecasts.

A combination of the VAR and ICF forecast schemes is possible, but doing this did not combine the benefits from both schemes. Instead, it was better to use a Kalman filter with the identified model as an observer model in the VAR model forecast. This combination improved the short-term forecast of the VAR model considerably. Nonetheless, it did not perform equally well for all observed iceberg trajectories and sometimes it even degraded the forecast performance.

A comparison between the forecast performance of different icebergs should be performed with a relative performance index. This reveals how well the icebergs are forecasted relative to the velocity of the iceberg. About 70 % to 90 % of all forecasts performed by the statistical forecast models are classified as acceptable or better. This means the forecast error is at least in the same range as the drift distance of the iceberg in the period.

For future work a potential method to improve the iceberg drift forecast is by changing between different forecast methods, which are specialized for different forecast horizons. This change has to be performed by using the forecasted iceberg velocity from different models. For example, the ICF model is used up to a forecast horizon of 12 h, and for longer forecasts the position is used to initialize the VAR model.

Another possible improvement may be achieved by creating a more complex model for the ICF forecast scheme that not only considers the inertial current but also includes tidal currents explicitly in the observer model.

A further interesting research question is how well the relative forecast performance for longer forecast horizons can be predicted based on a 1 h, 3 h and 6 h forecast. Is it possible to classify a priori some forecasts as not trustworthy and how high is the success-rate of this classification?

Acknowledgement

The authors would like to thank Statoil, ArcticNet and the CCGS *Amundsen* for contributing to a safe Offshore Newfoundland Research Expedition 2015. We also thank NSERC and ArcticNet for funding and assistance with deployment of the iceberg trackers. This work was supported by Statoil ASA, and in part by Centre for Autonomous Marine Operations and Systems (CoE AMOS, RCN project no. 223254). We also want to thank the three anonymous reviewers for their comments which helped to greatly improve this paper.

Table 15: Mean end-position-error (17) [km] for different forecast horizons of all iceberg for each method considered in the article. The standard deviation is given in brackets and the best forecast is marked bold. The static model gives an indication the iceberg drift distance within the forecast horizon. The VAR KF and ICF VAR are the two new forecast methods

	1 h	6 h	12 h	18 h	24 h
CVF	0.53 (0.41)	3.1 (2.6)	5.8 (4.9)	9.4 (7.5)	13.2 (10.3)
ACF	0.27 (0.21)	2.8 (1.9)	5.3 (3.9)	8.5 (6.1)	12.0 (8.7)
TCF	0.28 (0.22)	2.8 (2.0)	5.3 (4.3)	8.4 (6.3)	11.9 (8.9)
ICF	0.23 (0.19)	2.3 (1.6)	**4.6** (3.5)	7.4 (5.7)	10.5 (8.2)
VAR	0.49 (0.37)	2.6 (2.0)	**4.6** (3.7)	**7.2** (5.6)	**9.9** (7.6)
MEMD	**0.20** (0.15)	3.1 (2.2)	6.0 (4.5)	9.8 (7.2)	12.9 (11.5)
VAR KF	0.29 (0.22)	**2.2** (1.5)	4.7 (3.6)	7.6 (5.7)	10.9 (8.0)
ICF VAR	0.25 (0.20)	2.4 (1.9)	5.2 (5.0)	8.2 (7.4)	11.4 (10.7)
DYM	0.54 (0.38)	3.7 (2.6)	7.1 (5.0)	10.5 (7.3)	13.7 (9.3)
STAT	0.82 (0.51)	4.6 (2.9)	8.6 (5.3)	12.7 (7.5)	16.4 (9.8)

Appendix A. Extension to the Comparison of Iceberg Drift Forecasts

This appendix shows the iceberg drift trajectories of each iceberg, and the progression of the 12 h forecast error for some of the methods presented in the article.

Appendix A.1. Iceberg 1

In Tab. 5 the mean and standard deviation of the forecast methods are shown. The MEMD forecast scheme produces the best forecast within the first hour. For six hours the ancillary forecast scheme is the best. For longer forecast horizons the VAR forecast scheme produces the best results. If the PI (19) is considered the ancillary forecast scheme produces a better result than the VAR forecast scheme for a 12 h forecast.

Besides the CVF all methods are superior to the dynamic forecast model up to a forecast period of 12 h. For longer forecast horizons (18 h and 24 h) the TCF, MEMD and CVF schemes produce a larger average error than the dynamic model.

Interestingly, the standard deviation relative to the mean error is smaller for the dynamic forecast model compared to the statistical methods indicating that the statistical methods have a larger spread in the forecast errors.

The end-position error of a 12 h forecast of every method is shown in Fig. A.8a. The corresponding iceberg trajectory is shown in Fig. A.8b. The large standard deviation of the statistical methods (Tab. 5) are caused by the large error in the period 60 h to 85 h. This is the period where the iceberg enters the first large loop. The forecast error is also large when the iceberg exists the loops. These loops have a period of about 18 h to 24 h. The ocean eddies causing the looping are most likely provoked by the current flows in and out of Conception Bay (between Grates Cove and Bonavista (Fig. 2)).

The error progressions of the methods, besides the dynamic and static model, are similar. The static model serves as a reference to the iceberg drift velocity. The forecast performance is not good since the static model is often better than the other models (Fig. A.8a). All methods rely on a similar principle, which makes it difficult to predict strong unexpected changes. Oscillations caused by tidal or inertial current can be forecasted by the ICF, VAR and MEMD forecast models.

The main advantage of the VAR model compared to the other methods is the reduction of the error between 70 h to 120 h. In this period the dynamic model also performs well, since it is able to forecast the second loop. On the other hand, the exit from the loop is forecasted by neither the dynamic nor statistical models.

Appendix A.2. Iceberg 4

In Tab. 6 the mean and standard deviation of the forecast methods are shown. The MEMD forecast scheme performs best in the first hour. Thereafter, the VAR forecast scheme is best.

The end-position error of a 12 h forecast of the VAR, ICF and dynamic forecast model is shown in Fig. A.9a. The corresponding iceberg trajectory is shown in Fig. A.9b. Larger errors in the statistical models are produced before the iceberg enters the curves at about 193 h and 289 h. These are not anticipated by the forecasts.

The statistical models behave similarly. The VAR model is superior to the ICF model especially in the second part of the observed iceberg trajectory. The forecast of the iceberg drift of Iceberg 4 with the statistical methods is good, and the error compared to the dynamic forecast model can be reduced considerably. For only a few short periods the dynamic model performs better than the statistical model forecast (Fig. A.9a).

Appendix A.3. Iceberg 4-3

In Tab. 7 the mean and standard deviation of the forecast methods are shown. The MEMD forecast scheme performs best in the first hour. Thereafter, up to a forecast horizon of about 12 h the ICF scheme performs best. For longer forecast horizons up to 24 h the VAR model forecast is the best. The dynamic forecast model outperforms the CVF, TCF and MEMD scheme already after 12 h.

The end-position error of a 12 h forecast of the VAR,

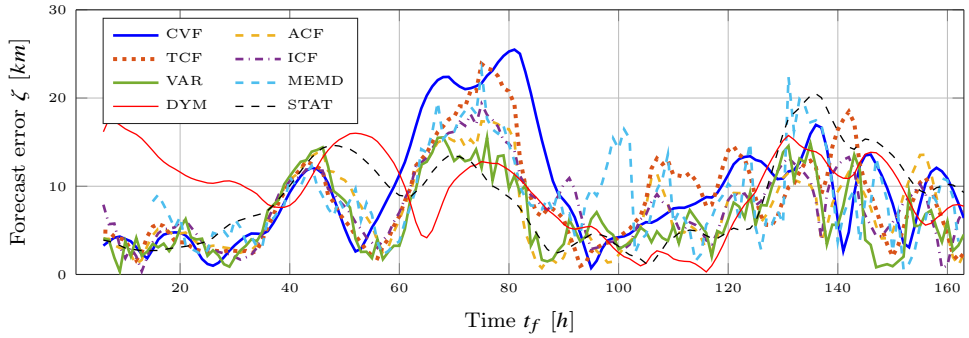

(a) Forecast error for different forecast schemes with a forecast horizon of 12 h for Iceberg 1.

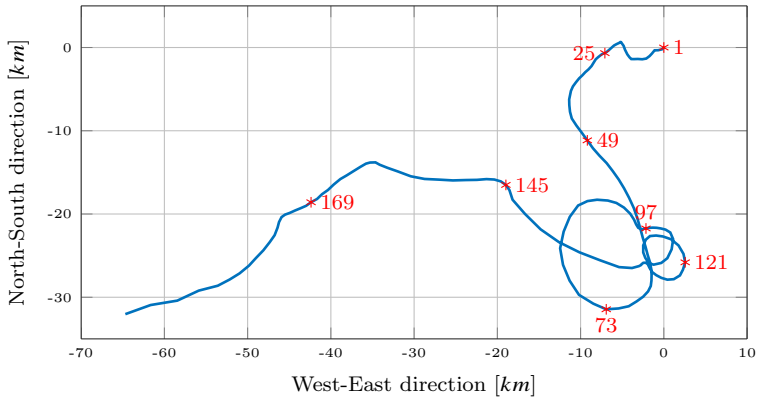

(b) Iceberg drift trajectory of Iceberg 1. The number marker corresponds to the time t_f in the upper figure.

Figure A.8: Forecast results for Iceberg 1. The forecast error is shown in the upper figure, while the lower figure shows the corresponding iceberg drift trajectory.

ICF and DYM model is shown in Fig. A.10a. The corresponding iceberg trajectory is shown in Fig. A.10b. The rapid changes in iceberg velocity and direction causes the strong oscillation in the forecast performance. This is also amplified by the squeezed x-axis.

The dynamic model has a similar performance as the statistical forecast methods. In the comparison of both approaches it can be observed that at the beginning (0 h to 250 h) the statistical models perform better, in the middle part (250 h to 500 h) the dynamic model performs better and in the end the statistical models perform again better.

Iceberg 4-3 is believed to be relatively small, which enables it to move relatively quickly. Consequently, the statistical models do not outperform the dynamic model by much. A similar observation was already made for the forecast of Iceberg 1, which had several unexpected loops in its trajectory.

Appendix A.4. Iceberg 1040-1

In Tab. 8 the mean and standard deviation of the forecast methods are shown. The MEMD forecast scheme is the best in the first hour, but for longer forecast horizons (6 h to 24 h) the ICF scheme is the best. For longer forecast horizons the dynamic model outperforms the MEMD (18 h to 24 h) and the CVF (24 h) scheme. All other statistical forecast schemes are better than the dynamic model.

The end-position error of a 12 h forecast of the ACF, ICF and dynamic forecast model is shown in Fig. A.11a. The corresponding iceberg trajectory is shown in Fig. A.11b. The loops at the beginning of the observation and the left-turn at about 200 h are not well forecasted by the statistical model. The drift to the south (about 230 h to 370 h), on the other hand, is relatively well forecasted. In this period the fast frequencies (tidal and inertial current) are less important, since the overall iceberg velocity is relatively large.

The dynamic iceberg model does not forecast the iceberg track well at the beginning (1 h to 130 h), since both ocean current and wind do not correlate with the iceberg velocity. In the period 130 h to 180 h the iceberg is mainly wind driven, since the ocean current velocity is very small (close to zero). The loops observed in this period correlate with the current velocity, but the amplitude of the oscillation is damped in the current velocity to about 40 % relative to the amplitude observed in the iceberg velocity. In the period 300 h to 480 h wind and current velocity correlate well with the iceberg velocity. The left-turn at about 380 h is anticipated by the input data, but about 6 h time-displaced. In fact, also in the period 480 h to 650 h the wind velocity correlates well with the iceberg velocity. The error in the forecast is caused by the ocean current.

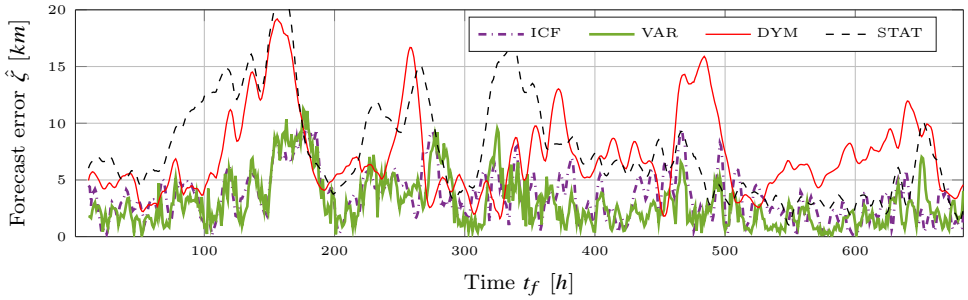

(a) Forecast error for different forecast schemes with a forecast horizon of 12 h for Iceberg 4.

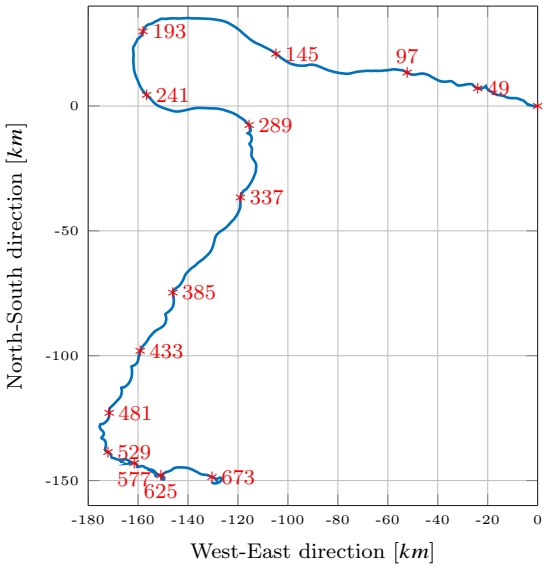

(b) Iceberg drift trajectory of Iceberg 4. The number marker corresponds to the time t_f in the upper figure.

Figure A.9: Forecast results for Iceberg 4. The forecast error is shown in the upper figure, while the lower figure shows the corresponding iceberg drift trajectory.

Overall the wind input correlates well with the iceberg velocity in the period 350 h to 800 h.

Especially in the middle part of the track (200 h to 650 h) the statistical models perform better than the dynamic model. At the end the dynamic model is slightly better.

Appendix A.5. Iceberg 1040-2

In Tab. 9 the mean and standard deviation of the forecast methods are shown. For a one hour forecast the MEMD forecast scheme performs best. For longer forecast horizons the TCF scheme is the best, closely followed by the ICF scheme. The MEMD and ACF scheme have a considerably larger forecast errors. Every statistical forecast method outperforms the dynamic forecast scheme. Indeed, the dynamic forecast model performs badly for this iceberg trajectory. The reason is a strong over-prediction of the ocean current velocity in the first 100 h (Fig. A.12a). Even though, the iceberg moves quickly in this period (average velocity 31 cm/s) the average velocity difference to the current velocity is about 45 cm/s.
The static model (STAT) indicates that the iceberg moves quickly in the entire observation period. Thus, the statistical models produce a larger error compared to some of the other icebergs, even though the iceberg trajectory is smooth without loops or sudden turns (Fig. A.12b).

The statistical models behave similar (Fig. A.12a). The dynamic model produces a very large error in the first 100 h, but in the period between 120 h to 200 h the dynamic model is slightly better than the statistical models. The two peaks (about 238 h and 276 h) in the forecast of the statistical models are caused by large measurement errors, which cause peaks in the iceberg velocity (to about 70 cm/s). It is due to transmission errors in the position data set of Iceberg 1040. In these two instances the error was not corrected since it would have needed post-processing, which was avoided in the comparison.

Appendix A.6. Iceberg 5450

In Tab. 10 the mean and standard deviation of the forecast methods are shown. For a one hour forecast the MEMD forecast scheme performs best. For a six hour forecast the ICF scheme is the best followed by the VAR forecast scheme. The latter also performs best for longer forecast

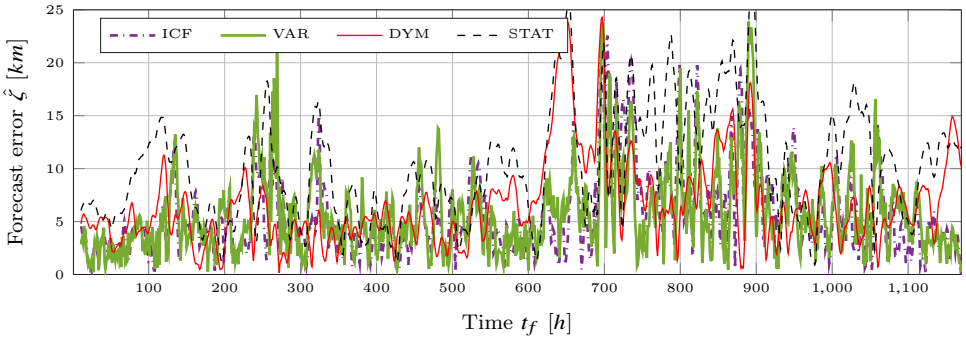

(a) Forecast error for different forecast schemes with a forecast horizon of 12 h for Iceberg 4-3.

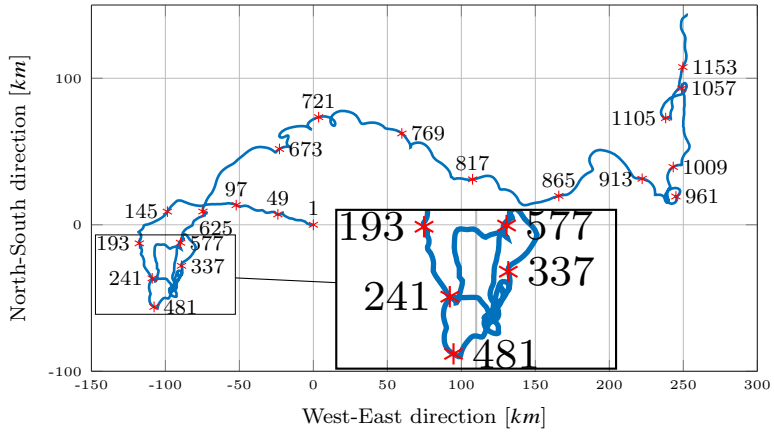

(b) Iceberg drift trajectory of Iceberg 4-3. The number marker corresponds to the time t_f in the upper figure.

Figure A.10: Forecast results for Iceberg 4-3. The forecast error is shown in the upper figure, while the lower figure shows the corresponding iceberg drift trajectory. The inset magnifies the part of the track that contains many loops and direction changes.

horizons (12 h to 14 h). All statistical models outperform the dynamic model, which has a similar forecast error as the static model.

The end-position error of a 12 h forecast of the ICF, VAR and dynamic forecast model is shown in Fig. A.13a. The corresponding iceberg trajectory is shown in Fig. A.13b.

The statistical models predict the movement of Iceberg 5450 well, even though the iceberg moves relatively quickly (average velocity about 21 cm/s). The dynamic forecast model, on the other hand, is not able to forecast the iceberg drift as well. It is outperformed by the statistical models over almost the entire observation period.

Appendix A.7. Iceberg 3534

In Tab. 11 the mean and standard deviation of the forecast methods are shown. The statistical forecast models outperform the dynamic one. Exceptions are the ACF and MEMD forecast schemes. The VAR and ICF, which perform best for different forecast horizons, have a similar forecast performance. The other statistical models cannot compete with them.

The end-position error of a 12 h forecast of the ICF, VAR and dynamic forecast model is shown in Fig. A.14a. The corresponding iceberg trajectory is shown in Fig. A.14b.

The statistical models perform for the most part of the observation period better than the dynamic model. This holds especially for the period 40 h to 130 h. Overall the forecast errors of the VAR and ICF model behave similarly, but it can be observed that the fast oscillations of the error are slightly different. Consequently, a combination of both forecast scheme would do even better. A similar behavior was also observed for the other icebergs.

Appendix A.8. Iceberg 3651

The end-position error of a 12 h forecast of the ICF, VAR and dynamic forecast model is shown in Fig. A.15a. The corresponding iceberg trajectory is shown in Fig. A.15b. The iceberg velocity increases strongly at the end of the observation period. This correlates with the forecast error. For this reason the standard deviation (Tab. 12) is also considerably larger than for Iceberg 3534 and Iceberg 5450.

The forecast performance of the statistical model is better than of the dynamic one. In fact, if only the first 200 h of the observation period are considered the 12 h mean forecast error is only about 1.36 km and the 24 h forecast error is about 3.95 km. This is a very small forecast error. The dynamic model also produces only a 3.3 km and 7.8 km error for a 12 h and 24 h forecast horizon, respectively. Again, the small absolute error is correlated

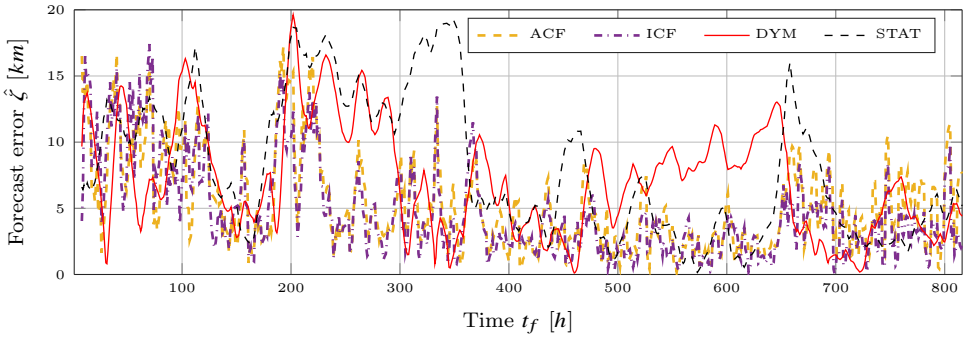

(a) Forecast error for different forecast schemes with a forecast horizon of 12 h for Iceberg 1040-1.

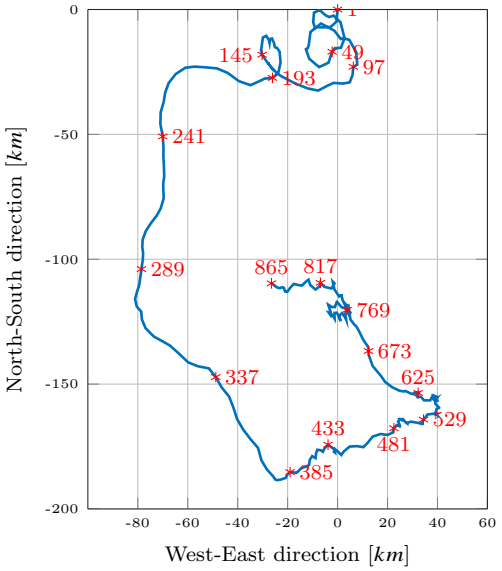

(b) Iceberg drift trajectory of Iceberg 1040-1. The number marker correspond to the time t_f in the upper figure.

Figure A.11: Forecast results for Iceberg 1040-1. The forecast error is shown in the upper figure, while the lower figure shows the corresponding iceberg drift trajectory.

with a small iceberg velocity during the period. Nonetheless, the strong oscillation in velocity causing small loops and a zigzag trajectory at the beginning of the observation does not influence the forecast negatively, since it is in the expected frequency of about 12 h. The loops at the beginning of the observation period are observed because of the small iceberg velocity. If the iceberg velocity is larger the inertial and tidal oscillations cannot be spotted so easily in the iceberg trajectory.

At about 210 h the velocity of the iceberg in both directions changes strongly. For this reason the forecast error increases strongly. The other large forecast error is due to the direction change at about 240 h. Obviously these changes are not explained by the wind and current data, which produces a large error in the dynamic model. In addition, the statistical models are not prepared for this sudden change, so they produce a large error.

References

Aftab, M. F., Hovd, M., Huang, N. E., Sivalingam, S., 2016. An adaptive non-linearity detection algorithm for process control loops. IFAC-PapersOnLine 49 (7), 1020–1025.

Andersson, L. E., Aftab, M. F., Scibilia, F., Imsland, L., 2017a. Forecasting using multivariate empirical mode decomposition – applied to iceberg drift forecast. In: IEEE Conference on Control Technology and Applications (CCTA), Kohala Coast, Hawaii.

Andersson, L. E., Scibilia, F., Imsland, L., 2016a. An estimation-forecast set-up for iceberg drift prediction. Cold Regions Science and Technology 131, 88–107.

Andersson, L. E., Scibilia, F., Imsland, L., 2016b. Estimation of systems with oscillating input - applied to iceberg drift forecast. In: IEEE Multi-conference on Systems and Control (MSC), International Conference on Control Applications (CCA), Buenos Aires. pp. 940–947.

Andersson, L. E., Scibilia, F., Imsland, L., 2016c. An iceberg drift prediction study offshore Newfoundland. In: Arctic Technology Conference, St. John's, Newfoundland and Labrador, Canada. Offshore Technology Conference.

Andersson, L. E., Scibilia, F., Imsland, L., 2016d. The moving horizon estimator used in iceberg drift estimation and forecast. In: European Control Conference (ECC), 2016. pp. 1271–1277.

Andersson, L. E., Scibilia, F., Imsland, L., 2017b. A study on an iceberg drift trajectory. In: ASME 2017 36th International

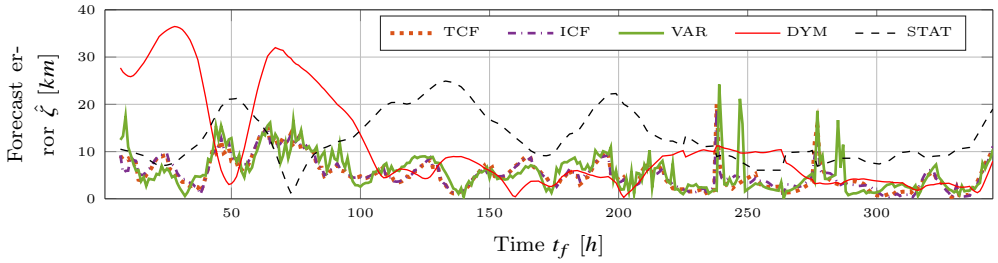

(a) Forecast error for different forecast schemes with a forecast horizon of 12 h for Iceberg 1040-2.

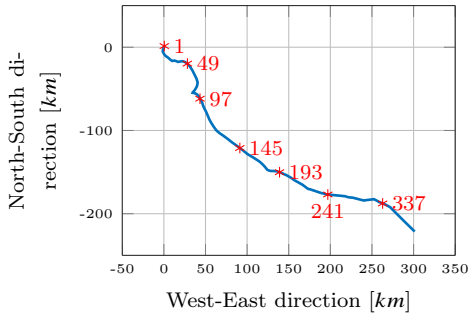

(b) Iceberg drift trajectory of Iceberg 1040-2. The number marker corresponds to the time t_f in the upper figure.

Figure A.12: Forecast results for Iceberg 1040-2. The forecast error is shown in the upper figure, while the lower figure shows the corresponding iceberg drift trajectory.

Conference on Ocean, Offshore and Arctic Engineering. Vol. 8. American Society of Mechanical Engineers, pp. V008T07A029–V008T07A029.

Andersson, L. E., Scibilia, F., Imsland, L., 2018. An iceberg forecast approach based on a statistical ocean current model. Cold Regions Science and Technology [submitted].

Barnett, L., Seth, A. K., 2014. The MVGC multivariate Granger causality toolbox: A new approach to Granger-causal inference. Journal of Neuroscience Methods 223, 50 – 68.

Bigg, G. R., Wadley, M. R., Stevens, D. P., Johnson, J. A., 1996. Prediction of iceberg trajectories for the North Atlantic and Arctic oceans. Geophysical Research Letters 23 (24), 3587–3590.

Bigg, G. R., Wadley, M. R., Stevens, D. P., Johnson, J. A., 1997. Modelling the dynamics and thermodynamics of icebergs. Cold Regions Science and Technology 26 (2), 113–135.

De Margerie, S., Middleton, J., Garrett, C., Marquis, S., Majaess, F., Lank, K., 1986. An operational iceberg trajectory forecasting model for the Grand Banks of Newfoundland. No. 52. Environmental Studies Revolving Funds.

De Young, B., Tang, C., 1990. Storm-forced baroclinic near-inertial currents on the grand bank. Journal of Physical Oceanography 20 (11), 1725–1741.

EI-Tahan, M., EI-Tahan, H., Venkatesh, S., et al., 1983. Forecast of iceberg ensemble drift. In: Offshore Technology Conference.

Eik, K., 2009. Iceberg drift modelling and validation of applied metocean hindcast data. Cold Regions Science and Technology 57, 67–90.

EU Copernicus Marine, 2006. [Online]. http://marine.copernicus.eu/. Available at: http://marine.copernicus.eu/services-portfolio/access-to-products/ [Accessed 23 Nov. 2017].

Garrett, C., Middleton, J., Hazen, M., Majaess, F., 1985. Tidal currents and eddy statistics from iceberg trajectories off Labrador. Science 227 (4692), 1333–1335.

Gaskill, H. S., Rochester, J., 1984. A new technique for iceberg drift prediction. Cold Regions Science and Technology 8 (3), 223 – 234.

GEBCO, -. [Online]. Available at: https://www.gebco.net/.

Granger, C. W., 1969. Investigating causal relations by econometric models and cross-spectral methods. Econometrica: Journal of the Econometric Society, 424–438.

Kubat, I., Sayed, M., Savage, S. B., Carrieres, T., 2005. An operational model of iceberg drift. International Journal of Offshore and Polar Engineering 15 (2), 125–131.

Kulakov, M. Y., Demchev, D. M., 2015. Simulation of iceberg drift as a component of ice monitoring in the West Arctic. Russian Meteorology and Hydrology 40 (12), 807–813.

Marko, J., Fissel, D., Miller, J., 1988. Iceberg movement prediction off the Canadian east coast. In: El-Sabh, M., Murty, T. (Eds.), Natural and Man-Made Hazards. Springer Netherlands, pp. 435–462.

McClintock, J., Bullock, T., McKenna, R., Ralph, F., Brown, R., 2002. Greenland iceberg management: Implications for grand banks management systems. PERD/CHC Report 20-65, AMEC Earth & Enviromental and C-Core, St. John's, NL.

Moore, M., 1987. Exponential smoothing to predict iceberg trajectories. Cold Regions Science and Technology 14 (3), 263 – 272.

Mountain, D., 1980. On predicting iceberg drift. Cold Regions Science and Technology 1 (3-4), 273 – 282.

Rawlings, J. B., Bakshi, B. R., 2006. Particle filtering and moving horizon estimation. Computers & Chemical Engineering 30 (10-12), 1529–1541.

Robertson, D. G., Lee, J. H., Rawlings, J. B., 1996. A moving horizon-based approach for least-squares estimation. AIChE Journal 42 (8), 2209–2224.

Scibilia, F., Hovd, M., 2009. Multi-rate moving horizon estimation with erroneous infrequent measurements recovery. In: Fault Detection, Supervision and Safety of Technical Processes. pp. 1037–1042.

Smith, S. D., 1993. Hindcasting iceberg drift using current profiles and winds. Cold Regions Science and Technology 22 (1), 33–45.

Sodhi, D., El-Tahan, M., 1980. Prediction of an iceberg drift trajectory during a storm. Ann. Glaciol 1, 77–82.

Turnbull, I. D., Fournier, N., Stolwijk, M., Fosnaes, T., McGonigal, D., 2015. Operational iceberg drift forecasting in northwest Greenland. Cold Regions Science and Technology 110, 1 – 18.

Ur Rehman, N., Mandic, D. P., 2010. Multivariate empirical mode decomposition. In: Proceedings of The Royal Society of London A: Mathematical, Physical and Engineering Sciences. Vol. 466.

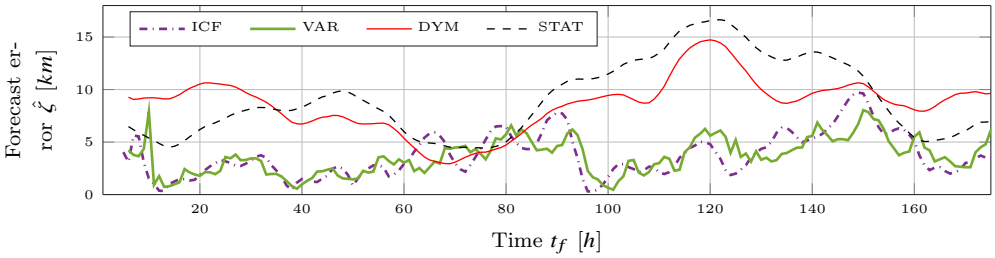

(a) Forecast error for different forecast schemes with a forecast horizon of 12 h for Iceberg 5450.

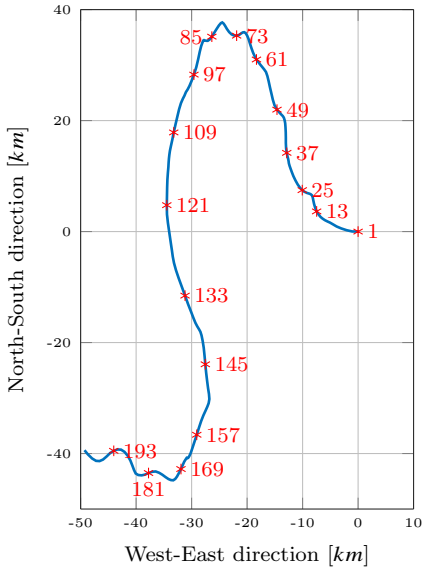

(b) Iceberg drift trajectory of Iceberg 5450. The number marker corresponds to the time t_f in the upper figure.

Figure A.13: Forecast results for Iceberg 5450. The forecast error is shown in the upper figure, while the lower figure shows the corresponding iceberg drift trajectory.

The Royal Society, pp. 1291–1302.
Wagner, T. J., Dell, R. W., Eisenman, I., 2017. An analytical model of iceberg drift. Journal of Physical Oceanography 47 (7).

Appendix B. List of figures

List of Figures

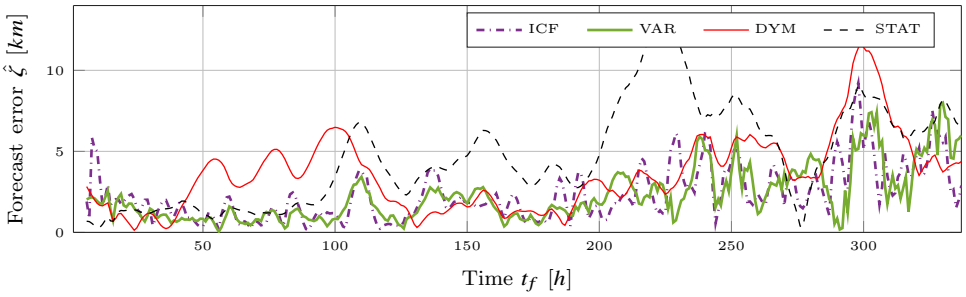

(a) Forecast error for different forecast schemes with a forecast horizon of 12 h of Iceberg 3534.

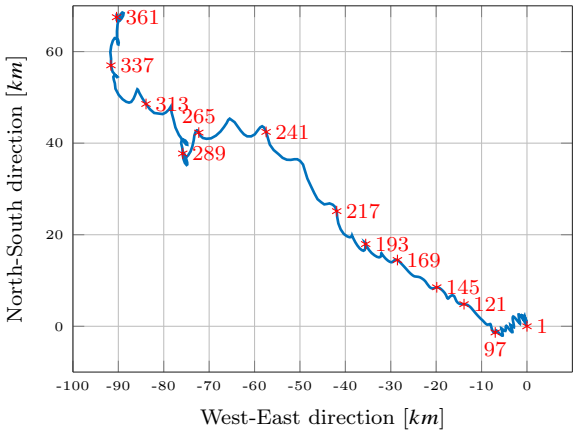

(b) Iceberg drift trajectory of Iceberg 3534. The number marker correspond to the time t_f in the upper figure.

Figure A.14: Forecast results of Iceberg 3534. The forecast error is shown in the upper figure, while the lower figure shows the corresponding iceberg drift trajectory.

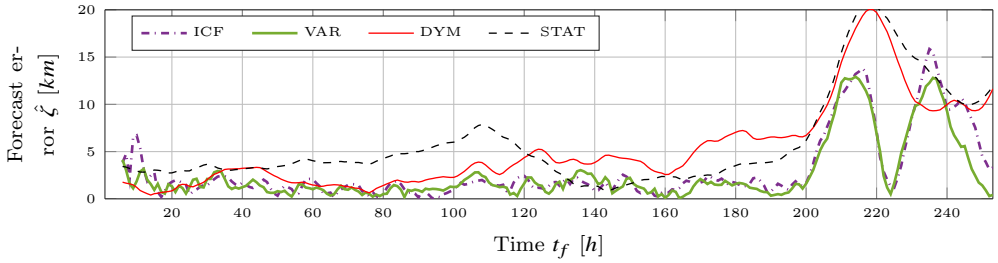

(a) Forecast error for different forecast schemes with a forecast horizon of 12 h of Iceberg 3651.

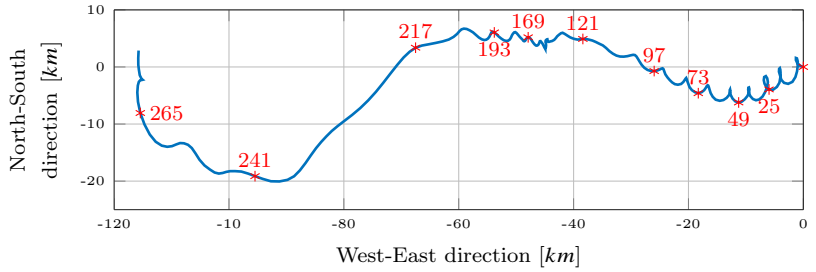

(b) Iceberg drift trajectory of Iceberg 3651. The number marker corresponds to the time t_f in the upper figure.

Figure A.15: Forecast results for Iceberg 3651. The forecast error is shown in the upper figure, while the lower figure shows the corresponding iceberg drift trajectory.

Appendix C. List of tables

List of Tables